Impacts of land-cover changes on snow avalanche activity in the French Alps

Robin Mainieri, Adrien Favillier, Jérôme Lopez Saez, Nicolas Eckert, Taline Zgheib, Pauline Morel, Mélanie Saulnier, Jean Luc Peiry, Stoffel Markus, Christophe Corona

Impacts of land-cover changes on snow avalanche activity in the French Alps

Robin Mainieri[1], Adrien Favillier[2,3,4], Jérôme Lopez-Saez[3,4], Nicolas Eckert[5], Taline Zgheib[5], Pauline Morel[1,5], Mélanie Saulnier[6], Jean-Luc Peiry[7], Markus Stoffel[3,4,8], Christophe Corona[2].

1. University Grenoble Alpes, IRSTEA, UR LESSEM, 2 rue de la Papeterie-BP76, F-38402 Saint-Martin-d'Hères, France

2. Université Clermont Auvergne, CNRS, Université de Limoges, GEOLAB, F-63000 Clermont-Ferrand, France

3. University of Geneva - Institute for Environmental Sciences, Climatic Change and Climate Impacts, 66 Boulevard Carl-Vogt –CH-1205 Geneva, Switzerland

4. Dendrolab.ch, Department of Earth Sciences, University of Geneva, rue des Maraîchers 13, CH-1205 Geneva, Switzerland

5. University Grenoble Alpes, IRSTEA, UR ETNA, 2 rue de la Papeterie-BP76, F-38402 Saint-Martin-d'Hères, France

6. Faculty of Forestry and Wood Sciences, Czech University of Life Sciences, Kamýcká 129, 16521 Prague, Czech Republic

7. CNRS, UMI3189, "Environnement, Santé, Sociétés", Faculté de Médecine, UCAD, BP 5005, DAKAR-FANN, Sénégal

8. Department F.-A. Forel for Environmental and Aquatic Sciences, University of Geneva, 66 Boulevard Carl-Vogt, CH-1205 Geneva, Switzerland

Impacts of land-cover changes on snow avalanche activity in the French Alps

Abstract

Dendrogeomorphic analyses provide long and continuous chronologies of mass movements that are useful for the detection of trends related to climate change. Socio-environmental changes can, however, induce non-stationarities. This study addresses the following questions: (1) How does the evolution of forest cover induce non-stationarities in tree-ring based reconstructions of snow avalanche activity? (2) How are trends inherent to tree-ring approaches distinguishable from real fluctuations in avalanche activity? Using dendrogeomorphic techniques, we reconstructed snow avalanches in six adjacent paths in the French Alps. Results show two distinct trends in process activity between 1750 and 2016. In the southern paths, the frequency of snow avalanches increased sharply in the 1970s. The distribution of tree ages, as well as old topographic maps, allow an attribution of this trend to the destruction of large parts of the forest stand by a large snow avalanche in the 1910-20s. This extreme event induced a sudden change in the capability of newly colonizing trees to record subsequent snow avalanches. In the northern paths, by contrast, progressive afforestation starting in the mid-19th century, as well as colonization of the release areas after World War II, resulted in a strong reduction in snow avalanche activity since the 1930s. Even if global warming remains a possible additional driver of snow avalanche activity at the study sites, the rural exodus and the abatement of pastoral practices during the 19th and 20th centuries are the main explanations for the observed trends in process activity. Results also illustrate a need to clarify the complex interrelations among forest evolution, global warming, social practices, and the process activity itself when interpreting trends in mass movements.

Keywords: Snow avalanches, tree-ring analysis, land cover changes, French Alps

1. Introduction

Climate warming in Europe has occurred since the end of the Little Ice Age (or LIA) around ~1850; this trend has accelerated more markedly since ~1985 (IPCC, 2013). High mountain environments experience a stronger response to climate change with even faster average warming as compared to the global mean (Mountain Research Initiative EDW Working Group et al., 2015). This evolution has resulted in rapid changes in the cryosphere (Beniston et al., 2018) and related changes in hydro-geomorphic process activity (Stoffel and Huggel, 2012). As a result of ongoing warming, available *in situ* snow depth data indicate an elevation-dependent decreasing trend in snow amounts, snow cover duration and snow water equivalent in the Alps (e.g. Bormann et al., 2018; Falarz, 2004; Laternser and Schneebeli, 2003; Marty et al., 2017; Morán-Tejeda et al., 2013). At the same time, the abandonment of traditional farming systems since the mid-19th century have affected many mountain regions across Europe, and even more so after World War II. The abatement of traditional farming has favored grassland abandonment,

subsequent forest encroachment (Gellrich et al., 2007; O'Rourke, 2006), and the progressive disappearance of mosaics of landscape features reflecting traditional mixed farming management (MacDonald et al., 2000).

Changes in snow cover characteristics often induce changes in spontaneous avalanche activity (Castebrunet et al., 2012; Stoffel and Corona, 2018), including alterations in friction and flow regime (Naaim et al., 2013; Köhler et al., 2018). Tree-ring and historical archives enable inferences of longer-term changes of avalanche activity (Corona et al., 2013; Giacona et al., 2017), and possibly detections of the impacts of climate change on snow avalanche activity. In this regard, Ballesteros-Cánovas et al. (2018) reported increased avalanche activity on some slopes of the Western Indian Himalaya over the past decades and related the changes in process behavior to the increased frequency of wet-snow conditions. In the European Alps, studies have demonstrated negative correlations between past changes in avalanche numbers and runout distance, as well as avalanche activity in forested areas, with temperature changes. They have also shown positive correlations with snow depth changes (Eckert et al. 2013, Teich et al., 2012). These studies also suggested that avalanche mass and run-out distance have decreased over past decades, with a decrease of avalanches with a powder part since the 1980s, a decrease of avalanche numbers below 2000 m, but an increase of snow avalanches at higher elevations (Eckert et al., 2013; Lavigne et al., 2015; Gadek et al., 2017). At the same time, other studies have shown a positive trend in the proportion of avalanches involving wet snow over the last decades and for the months of December through to February (Pielmeier et al., 2013; Naaim et al., 2016).

A large body of literature has documented interferences between snow avalanche activity and land cover changes (e.g., Bebi et al., 2009; Germain et al., 2005; Hétu et al., 2015; Kulakowski et al., 2006, 2011; Podolskiy et al., 2014; Schneebeli and Bebi, 2004; Teich et al., 2012). Germain et al. (2005) showed that deforestation and landscape heterogeneity should be carefully considered as tree removal—after clear-cuts and forest fires—affected snow redistribution, which in turn would increase the frequency of events in existing and new avalanche paths. Similarly, Kulakowsky et al. (2011) demonstrated a decreasing fragmentation of forest stands on avalanche paths resulting from the modification of the disturbance regime interacting with land use changes and global warming over the last 45 years in Switzerland. Accordingly, changes in traditional agricultural systems are susceptible to affect avalanche activity, as they can favor passive colonization of release areas with shrubs and trees, with potentially marked consequences on avalanche frequency and on runout distances. Yet, to date, research has not considered the impact of land abandonment and marginalization on mass-movement activity in a thorough manner. One exception is the study of García-Hernández et al. (2017) who reported passive reforestation as the main driver of changes in avalanche damage in the Spanish Pyrenees over the last fifty years. Similarly, Giacona et al. (2018) reported that progressive land abandonment and decreased anthropogenic pressure have significantly reduced the exposure of properties (i.e. high-altitude farms in particular) to the risk of avalanches in the Vosges massif.

The lack of long-term studies is usually attributed to the scarcity of continuous records of past avalanche activity (see Corona et al., 2012). On wooded paths, dendrogeomorphology (Alestalo, 1971) allows to identify and date of growth disturbances induced by past mass-movement activity in ring-width series. It can therefore also provide continuous, annually resolved snow avalanche reconstructions to complement historical sources. Dendrogeomorphic approaches have repeatedly yielded reconstructions of multi-decadal to multi-centennial chronologies of snow avalanche events over the last decades in numerous mountainous regions worldwide (see Favillier et al., 2017 for a recent review). Yet, non-stationarities in process or site characteristics are likely to affect dendrogeomorphic reconstructions that will then impact the resulting time series of past events and trends therein. For this reason, Corona et al. (2012) proposed to adjust thresholds aimed at detecting past process activity in tree-ring records to account for the reduced frequency of reconstructed events related to the decreasing number of living trees back in time. Similarly, Favillier et al. (2018) attributed the over-representation of avalanche events in their reconstructions since the mid-20th century to the difficulty to retrieve ancient hidden scars (Stoffel and Perret, 2006), invisible on the stem surface, thus rendering the determination of suitable sampling positions a difficult task (Trappmann and Stoffel, 2013). Finally, age- and diameter-dependent sensitivities of trees observed in hydro-geomorphic processes are yet another factor to be considered (Tichavský and Šilhán, 2016). These sensitivities thus represent a third source of non-stationarity in tree-ring reconstructions.

In this study, we deployed a dendrogeomorphic approach to study snow avalanches on a slope of the upper Guil valley (Chateau-Ville-Vieille municipality, French Alps) in the Queyras massif. We addressed the following questions: (i) How does the forest cover evolution induce non-stationarities in tree-ring reconstructions of snow avalanche activity? (ii) How are trends inherent to tree-ring approaches distinguishable from real fluctuations in avalanche activity? To answer these questions, we selected a slope comprising six different avalanche paths with similar morphology (in terms of altitude of the starting zone and path length) but different forest cover (i.e. densely forested paths upstream and corridors characterized by a marked transverse zonation downstream), thus allowing comparison between reconstructions. To this end, we performed a diachronic analysis of historical maps, aerial photographs and estimated tree ages to document the evolution of the forest stand within each path. We hypothesized that potential non-stationarities in tree-ring reconstructions could result from (1) forest recolonization after destructive avalanche events or (2) afforestation related to recent socio-environmental changes at the study site.

2. Study site

The site under investigation is on the territory of Château-Ville-Vieille (Queyras massif, French Alps), 1.5 km to the northwest of a hamlet called Souliers. The study site is locally known as Grand Bois (44° 47'N, 6° 46'E, Fig. 1) and consists of a west-facing slope (135 ha) extending from the Crépaud ridge (2580 m asl) to the Souliers torrent (1900 m asl). Naturally triggered snow avalanches are common on the slope and release from several starting zones

97 located between 2300 and 2580 asl. We delineated six avalanches paths (S1-S4, A1-A2) based on the mapping of
98 erosional and depositional avalanche features in the field as well as on the interpretation of aerial photographs. We
99 derived the morphometric characteristics of each path from a 5-m Digital Elevation Model (DEM) extracted from the
100 IGN RGE ALTI® database (Tab. 1). With respect to land cover, a preliminary analysis of aerial photographs shows
101 a north-south gradient of afforestation on the selected paths, meaning that the forest cover increases from 31.2%
102 at A2 to 65.1% at S2. Paths S3-S4 and A1-A2 have characteristic transverse vegetation patterns, as defined by
103 Malanson and Butler (1984): dense shrubs with flexible stems colonize the inner zone of these paths, including
104 European rowan (*Sorbus aucuparia* L.) or common juniper (*Juniperus comunis*); in the outer zones, European larch
105 (*Larix decidua* Mill.) is dominant. Rhododendron (*Rhododendron ferrugineum* L.) and bilberries (*Vaccinium myrtillus*
106 L.) form most of the understory vegetation. By contrast, transverse vegetation patterns were absent at S1-S2 and
107 tree stand physiognomy (i.e. candelabra-shaped or broken-crown trees) was the main evidence of past avalanche
108 occurrences. According to Saulnier (2012), residents exploited the Grand Bois de Souliers slope intensively for
109 pastoralism since the mid-19th century. Despite a sharp decline in pastoral activities, forest exploitation remained
110 in place over large parts of the 20th century and until pastoralism disappeared in 1971 (Saulnier et al., 2015).

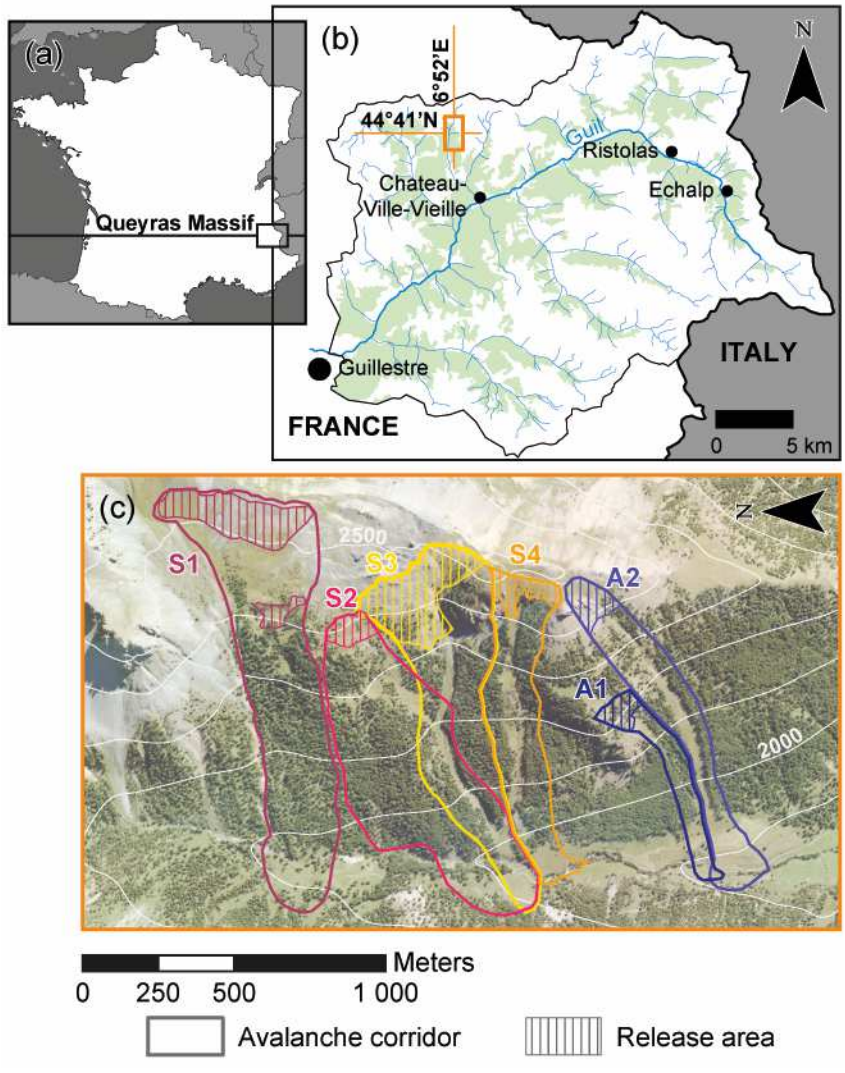

111

Figure 1. Location of the studied paths: (a) overview of the Queyras massif (French Alps), (b) detailed view of the Chateau-Ville-Vieille locality within the Queyras massif and the study site (c) detailed view of the six avalanche paths delineated on the Grand Bois de Souliers slope.

At the meteorological station of Saint-Véran (44°41'N, 6°52'E, 2039 m asl), located 12 km southeast of Grand Bois, mean annual precipitation and temperature are 709.6 mm and 5.3°C (1981–2010), with a winter (Dec-Apr) mean temperature of -0.2°C and winter precipitation totaling 237 mm on average. Due to its remoteness and the lack of objects at risk, the northernmost portion (S1-S4) of the Grand Bois de Souliers slope has neither been included in the EPA (Enquête Permanente sur les Avalanches; Bourova et al., 2016; Mougin, 1922) database nor mapped in the CLPA (Carte de Localisation des Phénomènes Avalancheux; Bonnefoy et al., 2010). Conversely, in the case of paths A1-A2, CLPA maps exist for two events: one in 1972 covering the Souliers road and torrent over 80 m. The second record is from December 2008 when a powder-snow avalanche destroyed 50 m^3 of wood. The 2008 event occurred during an intense avalanche cycle that affected the Queyras between December 14 and December 17, 2008 (Eckert et al., 2010b). During this period, southerly atmospheric fluxes progressively evolved into an easterly return causing important snowfall for three days. Cold temperatures and drifting snow aggravated the situation and caused the occurrence of 209 avalanches over a period of 5 days according to the EPA avalanche database. Some avalanches had very long runout distances and exceeded the historical limits recorded in the CLPA (Gaucher et al., 2009).

Table 1. Main characteristics of the studied avalanche paths. Numerical values correspond to the areas delineated in Fig. 1c and derived from crossed a 5-m DEM.

	Avalanche path					**Release area**			
Path	Aspect	Length (m)	Mean width (m)	Area (ha)	Mean slope (°)	Forest cover in 2015 (%)	Release altitude (m)	Mean slope (°)	Area (ha)
S1	W	1231	250	39.1	22.4	45.92%	2390-2570	28.1	7.9
S2	W	990	350	35.6	24.8	65.13%	2350-2420	26.7	1.5
S3	W	1107	250	27.6	28	43.53%	2300-2515	31.1	7.5
S4	W	950	180	16.5	28.8	55.49%	2380-2490	29.6	2.1
A1	W-S	695	92	6.02	27	50.33%	2150-2250	34.4	1.2
A2	W-S	1105	160	15.6	28.4	31.20%	2375-2490	34.8	2

3. Material and methods

3.1. Sampling strategy, dating and classification of growth disturbances

The field work missions in summers 2011 (S1-S2) and 2016 (S3-S4, A1-A2) allowed collecting a total of 884 increment cores from 825 European larch (*Larix decidua* Mill.) trees growing in the 6 avalanche paths. In the field, the sampling design followed the recommendations of Šilhán and Stoffel (2015) and Stoffel and Corona (2014), with particular attention paid to the number and the spatial distribution of sampled trees as well as to the balance

between older and younger trees. The use of a 1-m precision GPS device allowed recording the position of each tree. In addition, we recorded a series of data including the diameter at breast height (DBH) and the nature of the disturbance (type, height) in the field. In the lab, we applied standard dendrochronological procedures (Stoffel and Bollschweiler, 2008) to process the samples. We used the Souliers and Echalp reference chronologies (Corona et al., 2012; Saulnier et al., 2019) to cross-date growth disturbances (GD) identified in the tree-ring series and to correct the tree-ring records of affected trees in case of missing or false tree rings. We considered injuries and callus tissues (CT) (Stoffel et al., 2010), tangential rows of traumatic resin ducts (TRD) (Schneuwly et al., 2009a, 2009b), compression wood (CW) and sharp growth suppression (GS; Kogelnig-Mayer et al., 2013)—considered if tree-ring width was ≥60% smaller over ≥3 year compared to mean tree-ring width of the 5 years preceding the sharp decrease—as the most reliable indicators of past avalanche activity. To emphasize features obviously associated to snow avalanche activity, we classified GDs by intensity (Stoffel et al., 2013) based on their visual aspect and according to the classification proposed by Kogelnig-Mayer et al. (2011) as follows: weak (intensity class 1), medium (intensity class 2), strong (intensity class 3) reactions and clear evidence of injuries (intensity class 4).

3.2. Detection of past avalanche events in growth disturbance series

To detect past snow avalanche events in GD series, we employed the four-step procedure proposed by Favillier et al. (2017); please refer to Fig. 2 for details. We restricted the avalanche reconstruction to the period for which at least 10 trees were alive. In addition, we adjusted the minimum number of GDs and Shroder's It index (Shroder, 1978) in a way to account for changes in sample depth (Butler and Sawyer, 2008; Corona et al., 2012). Definition of these thresholds depends on the nature of the avalanche path and the type of vegetation, and sometimes needs to be adjusted to the study site. For this reason, we employed thresholds that were less rigid than those proposed by Favillier et al. (2017) so as to (1) to maximize the frequency of reconstructed events while still (2) taking sufficient care not to include noise in the reconstruction. To optimize the reconstruction, we considered preferentially trees located in the release area and within the tracks for the reconstruction of snow avalanches. We added GDs observed in ring series of trees located in the runout zone of more than one avalanche path (S2–S3; Fig; 3a) as additional evidence of past events.

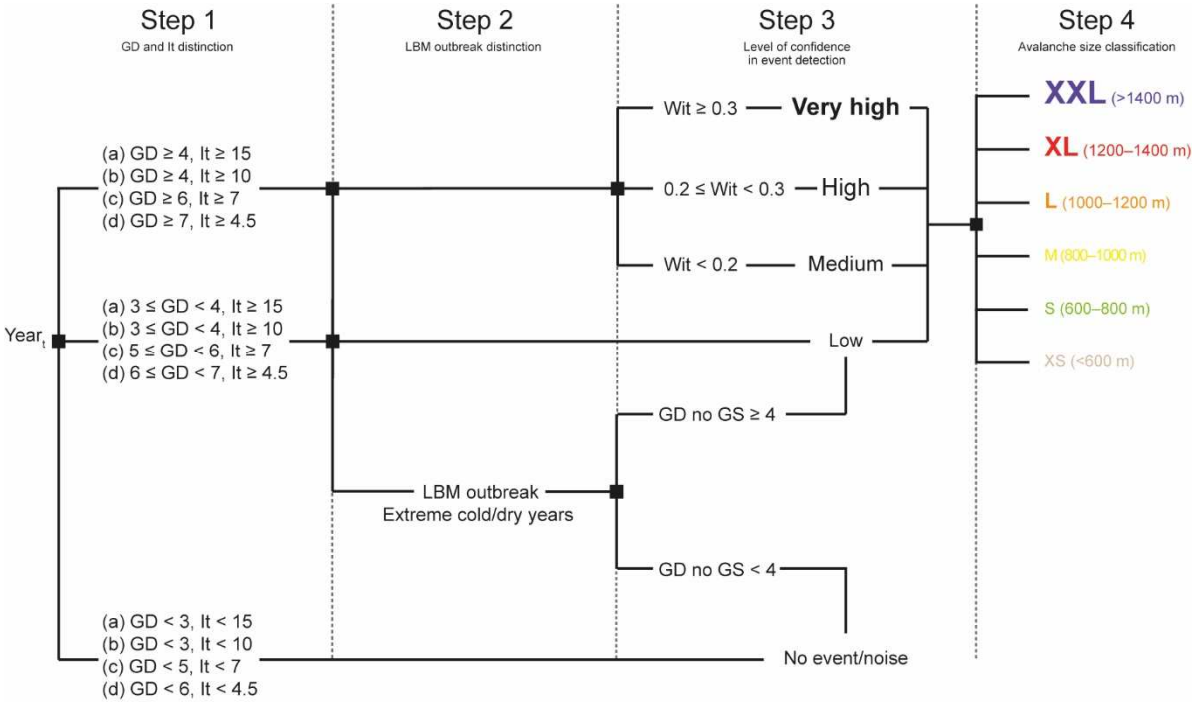

Figure 2. Synoptic diagram of the 4-step approach used for the detection of avalanche events in tree-ring series, adapted from Favillier et al. (2017). Growth disturbance (GD) and Shroder's It index (It) thresholds vary according to sample size: (a) <20 trees; (b) 20 to 49 trees; (c) 50 to 99 trees; and (d) ≥ 100 trees. We analyzed avalanche events occurring at the same time as larch budmoth outbreaks (LBM) or climatic events again and assigned confidence levels to this dating according to the weighted index factor (Wit).

In a second step (Fig. 2), we identified years with larch budmoth (LBM) outbreaks and climatic extremes (cold/dry years) as they could potentially bias the avalanche reconstruction. Saulnier et al. (2017) recorded LBM outbreak years at the study site. The homogenized temperature (1780-2014) and precipitation (1800-2002) records from the HISTALP grid points located nearest to the study site (Chimani et al., 2013; Efthymiadis et al., 2006) allowed the computation of extremely cold and dry summers. Table 2 presents the list of LBM events and extreme summers found at the study site. In case that potential avalanche events detected in step 1 coincide with LBM years or climatic extremes, we analysed tree-ring records again to avoid erroneous reconstruction of snow avalanches. In these years, we systematically excluded abrupt growth suppressions from the GD record. In addition, a minimum threshold of 3 GDs enabled the discrimination of avalanche from non-avalanche events (Fig. 2). In a third step, we assigned levels of confidence to each avalanche event based on the weighted index factor (Wit) proposed by Kogelnig-Mayer et al. (2011) accounting for GD type and intensity as follows: very high (vHLC, Wit > 0.3), high (HLC, 0.3 > Wit > 0.2) and medium (MLC, Wit < 0.2) (Favillier et al., 2017). To increase the stringency of the approach further, we rated each event detected during step 1 and events coinciding with LBM or climatic events in step 2 with a low level of confidence (LLC) (Fig. 2). In a last step, we mapped avalanche events and associated GDs using the ArcGIS 10.2.1 Time Slider (ESRI, 2013; Kennedy, 2013). On the basis of the position of impacted

trees, we categorized avalanches with a length <600 m, 600-800m, 800-1000m, 1000-1200m, 1200-1400m, and <1400 m as eXtra-Small (XS), Small (S), Medium (M), Large (L), eXtra-Large (XL), eXtra- eXtra-Large (XXL) avalanches, respectively. Fig. 2 summarizes the thresholds employed in the four-step procedure with respect to the minimal number of GDs, their intensity and the minimum percentage of disturbed trees. At the scale of individual paths, we computed the annual probability for an avalanche event by dividing the number of reconstructed events by the period covered by the reconstruction.

Table 2. Larch budmoth years (in bold) and pointer years (in italics) – according to Saulnier et al. (2017) – as well as extremely cold (*) and dry summers (**) (Efthymiadis et al., 2006; Saulnier et al., 2011) recorded in the French Alps. A careful analysis of these years enables detection of possible interferences between snow avalanche damage in trees and LBM and/or climatic signals. Both LBM and climate events may induce growth reductions comparable to those observed after snow avalanches in the tree-ring series.

2003**	*1926*	*1848*	*1801*
1997	*1925*	**1847**	**1795**
1996	*1918*	1843*	**1794**
1991**	1912*	1841*	*1779*
1980	**1910**	**1830**	*1766*
1972	*1909**	*1821**	*1758*
1963	1902	*1820*	*1750*
1950**	**1901**	1816*	
1947**	1888*	*1813**	
1945	*1867*	**1812**	
1937	1860*	*1803*	
1936	**1857**	**1802****	

3.3. Documentation of forest dynamics

Time series of cartographic documents are reliable indicators of spatio-temporal dynamics of forest stands (cadastral, topographic maps, aerial photographs; Houghton et al., 2012). In France, the oldest map yielding data on evolution is the Napoleonic cadastral map from the early 19th century. Specifically created for taxation purposes (Eynard-Machet, 1993), this map offers a precise and detailed record of land ownership and use at the level of allotments (Coughlan, 2013). At Souliers, the Napoleonic cadastral map dates to 1827. We used it as a baseline for the documentation of forest cover changes. In addition, we analyzed pictures from 5 aerial flight campaigns from the French National Geographic Institute (IGN; <1:30,000) to detect forest changes, namely in 1945, 1971, 1981, 2003 and 2015. Image interpretation was realized with standard photographic keys (i.e., tone, texture, pattern, shape, and size) and supplemented with secondary information on geomorphology, historical vegetation maps, and ground truth data. Based on these physiographic constraints, we realized visual interpretation and digitalization (Kennedy, 2013) at the path scale to generate maps of forest cover patterns for each of the dates, allowing

quantification of forest cover changes between 1945 and 2015 for each path and for 100-m elevation bands using ArcGIS 10.2.1 (ESRI, 2013). In addition, this analysis also investigated data from 11 aerial flight campaigns with lower-resolution images (>1:30,000) to detect evidence of high-magnitude snow avalanches that would have destroyed the forested stands partially between 1945 and 2016.

The age structure of the stand also served the assessment of forest dynamics for each path. For this purpose, we approximated the number of tree rings in each of the selected trees. Whenever the pith was not present on a core, we estimated the number of missing rings using the "*Estimate Distance and Rings to Pith*" function of the coo-recorder 9.0 software (Larsson, 2016). In this study, sampling positions ranged from 0.2 to 1.5 m above ground level. To compensate for the time elapsed from germination until a tree reaches sampling height, we added an age correction factor (Bollschweiler et al., 2008; Bosch and Gutiérrez, 1999; Muntán et al., 2004). We estimated age at sampling height in comparison to nearby *L. decidua* trees with according heights, for which the age could be easily determined by counting branch whorls (Sorg et al., 2010).

4. Results

4.1. Evolution of the forest cover

Trees sampled in the six paths were, on average, 186.1±126 years old. The oldest tree sampled in path S2 was 628 years old whereas the youngest tree (S3) reached sample height in 2010. Amongst the individuals sampled on the Grand Bois de Souliers slope, 40.6% of the sampled trees were less than 100 years old and 26.7% had between 200 and 300 growth rings at sampling height. One-fifth of all trees was older than 300 years (19.2%) and 8.3% of the sampled trees were at least 400-year-old. The spatial distribution of trees shows clear spatial patterns with three homogeneous areas (Fig. 3a): (1) an old-growth forest stand mainly composed of >300-year old trees in the northern part of the slope (S1-S2), (2) a cluster (S2-S3) where the distribution of tree ages ranges between 100 and 300 years but does not exceed 100 years at the margins of the main tracks, and (3) several clusters of senescent trees above 2200-2300 m asl.

Tree-ring data also provide valuable information on forest dynamics for the last century (Fig. 3a). Tree ages are significantly higher in paths S1 (306±122 yrs), S2 (229±122 yrs) and S3 (225±128 yrs) than in S4, A1 and A2 where tree ages averaged 137±120, 92±70 and 128±97 yrs, respectively. In paths S1-S3, sample depth exceeds 10% after 1620 CE and steadily increased between 1730 and 1860 (Fig. 3b). In these three paths, >70% of the sampled trees were present in 1860. Sample size evolved only moderately during the 20th century. By contrast, in paths S4 and A1-A2, sample size evolves moderately from 18.3, 5.5, and 14.3% in 1750 CE to 36.1, 16.9, and 33.6% in 1920, respectively. The number of sampled trees remains <40% before 1920 but sharply increases during the interwar period to exceed 80% after World War II. Here, results suggest a rapid colonization of the central part of the paths between the 1920s and the 1960s.

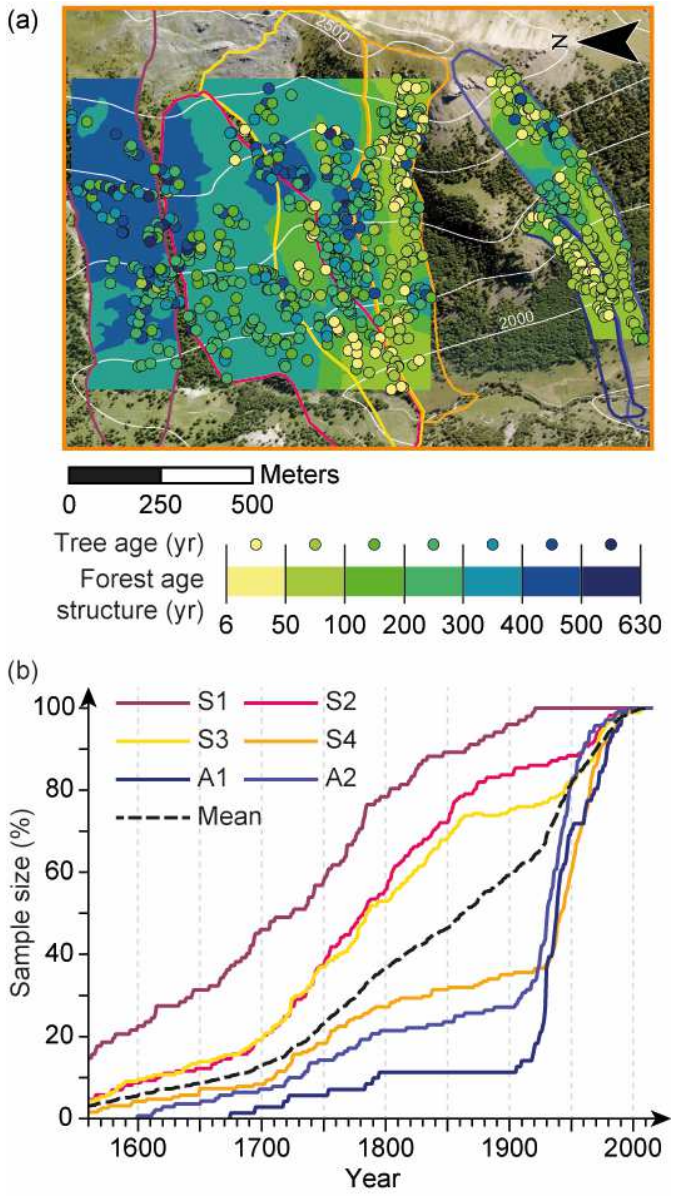

240

241 **Figure 3.** Age structure of the forest stand growing at Grand Bois de Souliers: (a) spatial distribution of individual
242 tree and interpolated stand ages; (b) evolution of the sample size at the six avalanche paths. The black line
243 represents the mean sample size evolution.

244 At the slope scale, historical maps and aerial photographs usefully supplement tree-ring data to document forest
245 evolution since the mid-19th century. At the Grand Bois de Souliers slope, the Napoleonian Cadastral map from
246 1827 shows a binary landscape with allotments (Getrille and Clos de la Chaussole) between 2100 and 2300 m asl
247 mainly occupied by larch stands, whereas rocks and scree covered with shrubs and herbs take over above 2300
248 m asl. Landscape changes appears rather limited between 1827 and 1945, but resolution obviously differs between
249 the cadastral map and the aerial photographs. Between 1945 and 1971 (Fig. 4), diachronic comparison of aerial
250 pictures reveals rapid forest sprawl, mostly in paths S1-S3, and an increase of forested areas between 2100 and
251 2300 m asl by 9 ha (+71.1%, Fig 5). In addition, the expansion of young trees on bare areas is clearly visible above

2300 m asl in S1-S3 (+0.72 ha). Between 1981 and 2015, forest colonization was ongoing above 2300 m asl (+9.6 ha), i.e. in a zone where avalanches are usually released. Over the full period covered by aerial pictures (1945–2015), the forested surface has more than doubled at Grand Bois de Souliers (32.7 vs. 89.7 ha or +274.3%).

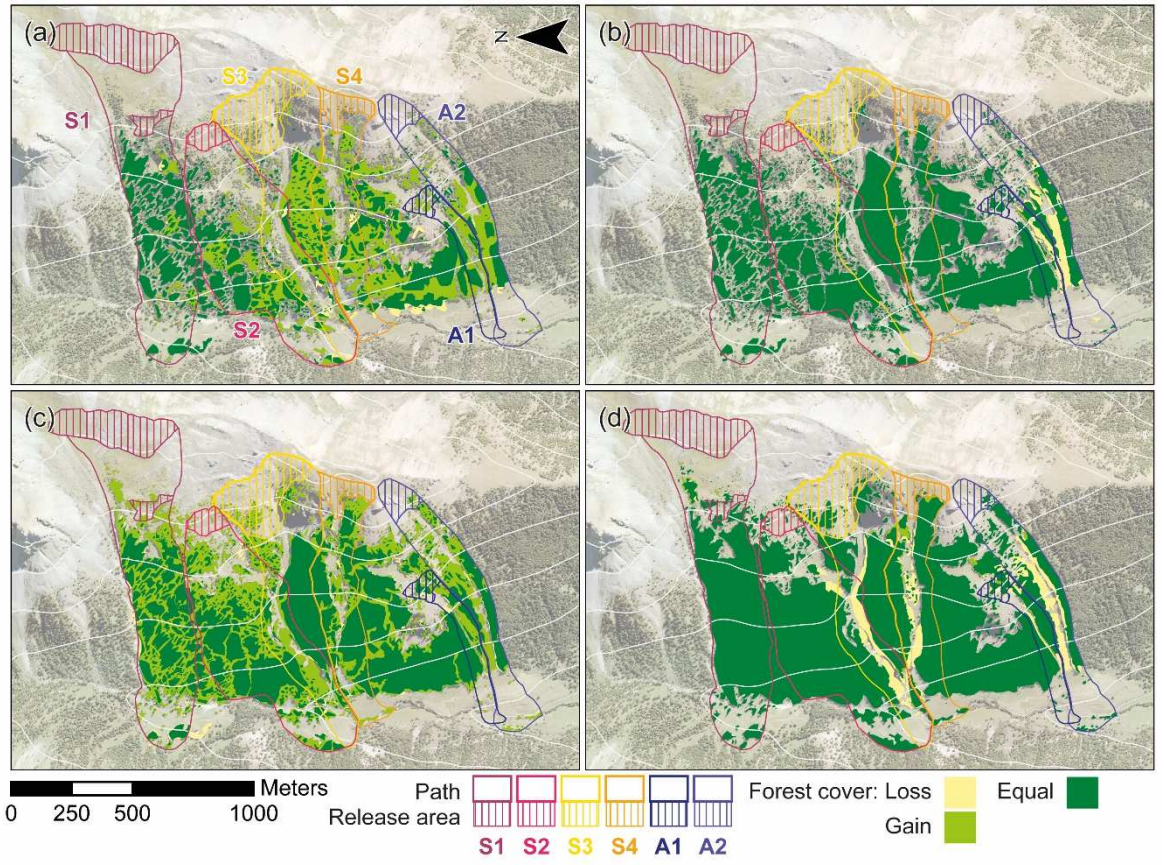

Figure 4. Diachronic evolution of the forest stands at Grand Bois de Souliers between 1945 and 2015: (a) 1945-1971, (b) 1971-1981, (c) 1981-2003, and (d) 2003-2015.

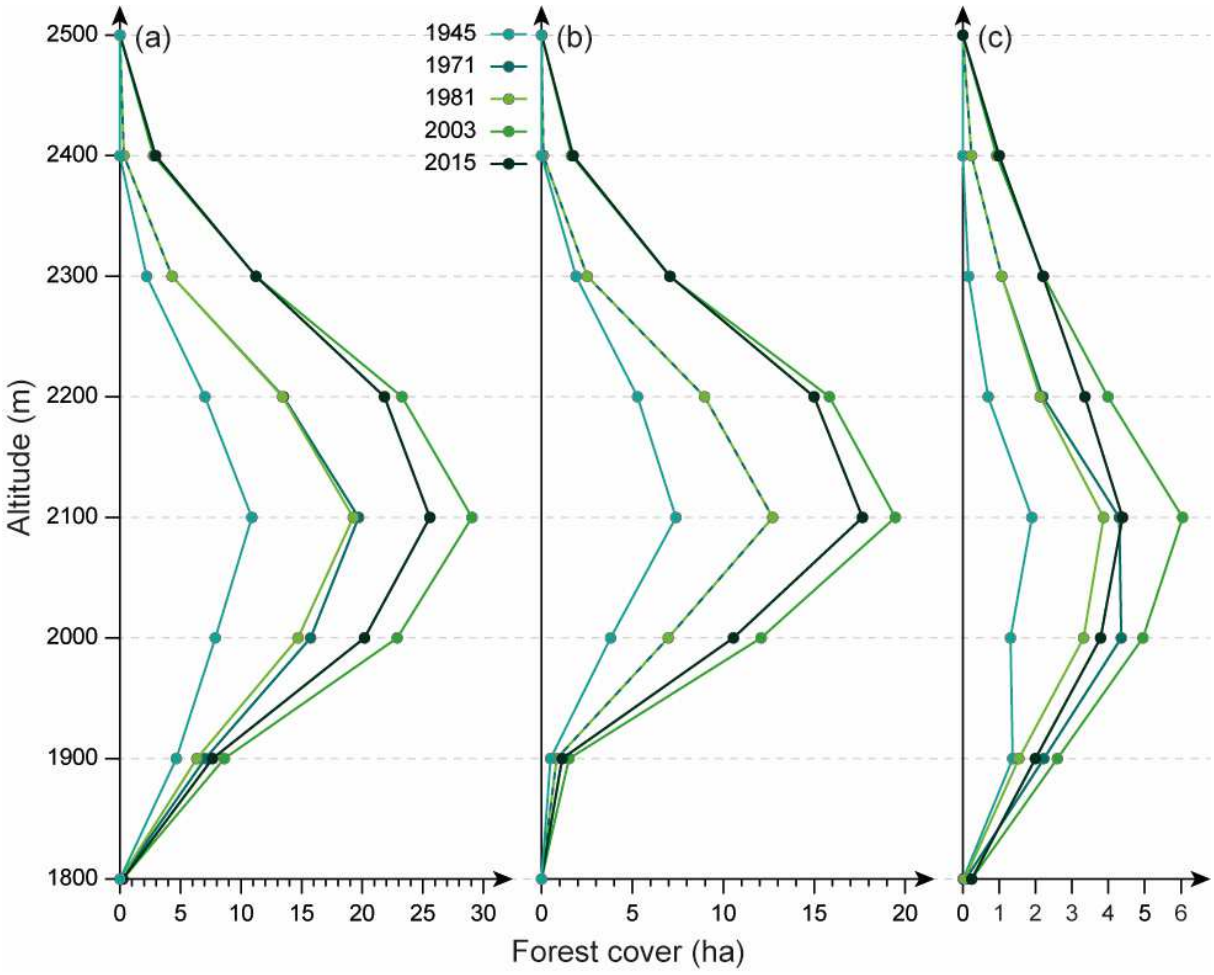

Figure 5. Evolution of the surfaces occupied by larch stands, computed for 100-m elevation bands, (a) at Grand Bois de Souliers; within (b) avalanche paths S1-S3; and (c) paths S4, A1 and A2 as delineated in Fig. 1.

4.2 Past snow avalanche activity

Comparison of the 16 additional aerial photographs available for the period 1945-2016 allowed retrieving signs of past avalanche events through the identification of avalanche-induced forest damage or avalanche deposits. Comparisons of aerial photographs of 1971–1974 and 2003–2009 allowed a delineation of the events listed in the CLPA for 1972 and 2008, respectively. We could not retrieve additional events in the 10 other photographs covering the periods 1945–1948, 1952–1971, 1974–2003, and 2009–2013 (Fig.4).

Analysis of the 825 trees sampled in the six paths allowed identification and dating of 2,460 GDs (1750-2016) with annual resolution. Table 3 summarizes the number and types of GDs identified at the slope and path scales. The mean number of GDs per tree is significantly lower in paths S1-S3 (1.85, 2.1, and 1.7 GD.tree^{-1}, respectively) as compared to paths S4, A1-A2 (3.7, 3.8, and 4.8 GD.tree^{-1}, respectively). Figure 6 shows types of GDs computed for the time windows 1750-1799, 1800–1849, 1850-1899,1900-1949, and 1950–1999 in paths S1-S3 (Fig. 6a) and S4-A1-A2 (Fig. 6b). In paths S1-S3, the mean number of GDs progressively decreased from 41.6 GD.decade^{-1} (n=208 GDs) in 1800-1849 to 28.2 GD.decade^{-1} (n=141 GDs) in 1950–1999. Conversely, in paths S4-A1-A2, we

detect a significant increasing trend from 20.4 GD.decade^{-1} (n=102 GDs) in 1750-1799 to 122.4 GD.decade^{-1} (n=612 GDs) in 1950–1999. For all paths, a clear shift is visible in the spectrum of mechanical damage: the percentage of growth suppression in the spectrum of mechanical damage decreased inversely proportional to the percentage of callus tissue, tangential rows of traumatic resin ducts and compression wood. In addition, in paths S4 and A1-A2, the proportion of injuries increased during the 19th century. Based on the 4-step procedure, the reconstruction of past events includes 974 GDs (40%). At the opposite, the procedure excluded 1460 GDs (60%) from analysis as they were noise and were not related to past snow avalanche activity. Amongst the 974 GDs, 314 had intensities of 3 or 4 are thus considered the more robust indicators of snow avalanching.

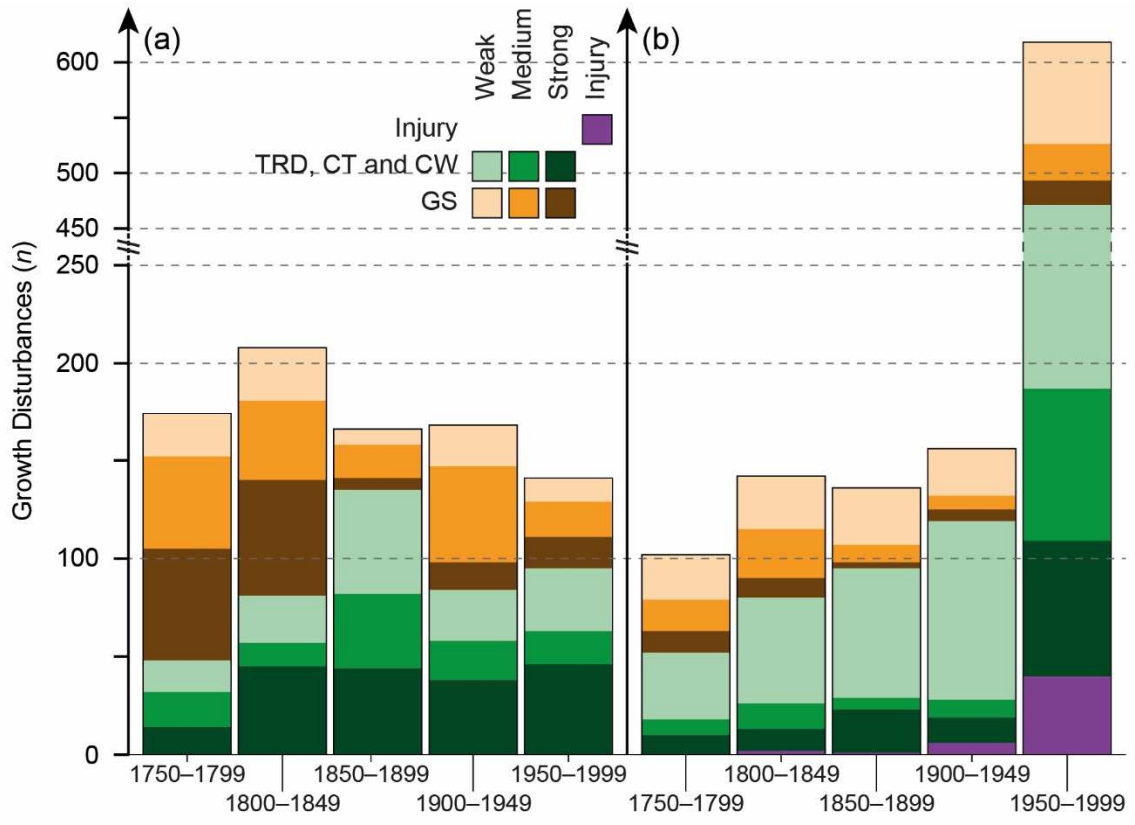

Figure 6. Bar plots showing the distributions of GD types and intensities between 1750 and 2000 for paths (a) S1-S3 and (b) S4-A1-A2.

Table 3. Intensities of reactions and types of growth disturbances (GD) assessed in the 825 larch trees selected for analysis.

Path	Impact scars (n)	Mechanical disturbances TRD, CT, CW (n)			Growth suppression (n)			Total
		strong	*medium*	*weak*	*strong*	*medium*	*weak*	
S1	0 (0%)	45 (1.8%)	11 (0.4%)	21 (0.9%)	57 (2.3%)	42 (1.7%)	13 (0.5%)	189 (7.7%)
S2	0 (0%)	70 (2.8%)	48 (2%)	88 (3.6%)	81 (3.3%)	96 (3.9%)	54 (2.2%)	437 (17.8%)
S3	0 (0%)	46 (1.9%)	17 (0.7%)	22 (0.9%)	31 (1.3%)	49 (2%)	26 (1.1%)	191 (7.8%)
S4	48 (2%)	80 (3.3%)	44 (1.8%)	218 (8.9%)	43 (1.7%)	86 (3.5%)	182 (7.4%)	701 (28.5%)

A1	4 (0.2%)	31 (1.3%)	32 (1.3%)	128 (5.2%)	12 (0.5%)	12 (0.5%)	53 (2.2%)	272 (11.1%)
A2	17 (0.7%)	84 (3.4%)	65 (2.6%)	305 (12.4%)	33 (1.3%)	55 (2.2%)	111 (4.5%)	670 (27.2%)
Total	69 (2.8%)	356 (14.5%)	217 (8.8%)	782 (31.8%)	257 (10.4%)	340 (13.8%)	439 (17.8%)	2460 (100%)

Dendrogeomorphic analysis allowed the dating of 97 snow avalanches (Fig. 7) occurring in 67 different years. Except for path A1 where the number of trees is insufficient to reconstruct avalanches before 1908, the sample depth exceeds the minimal threshold (n=10) for the period 1750-2016. In total, we reconstructed 6, 11, 11, 23, 10, and 36 avalanche events in paths S1, S2, S3, S4, A1 and A2, respectively. The oldest event occurred in 1756 on S2 whereas the most recent avalanche occurred in paths A1-A2 in 2015. Based on possible interferences between avalanche activity, climatic, and LBM signals in the tree-ring record (step 2), and based on the Weighted Index Factor (Wit; step 3, Figs. 7-8), we assigned very high and high levels of confidence to 28 and 30 events, respectively. By comparison, we reconstructed 22 events with a Wit<0.2, and characterized by a majority of weak and medium GDs, therefore rated with a LLC. We excluded 13 out of the 30 potential events coinciding with LBM outbreak episodes or extreme climatic years and we rated the 17 remaining events with an LLC (Fig. 7). At the annual scale, frequencies reached the highest values in the years 1808, 1908, 1933, 1971, 1972, 1984, and 2004, during which we reconstructed a snow avalanche on 3 out of 6 paths. Interestingly, we retrieved the two events mentioned in the CLPA for 1972 and 2008 with an LLC in S4-A1-A2 and with a vHLC in S4-A2, respectively.

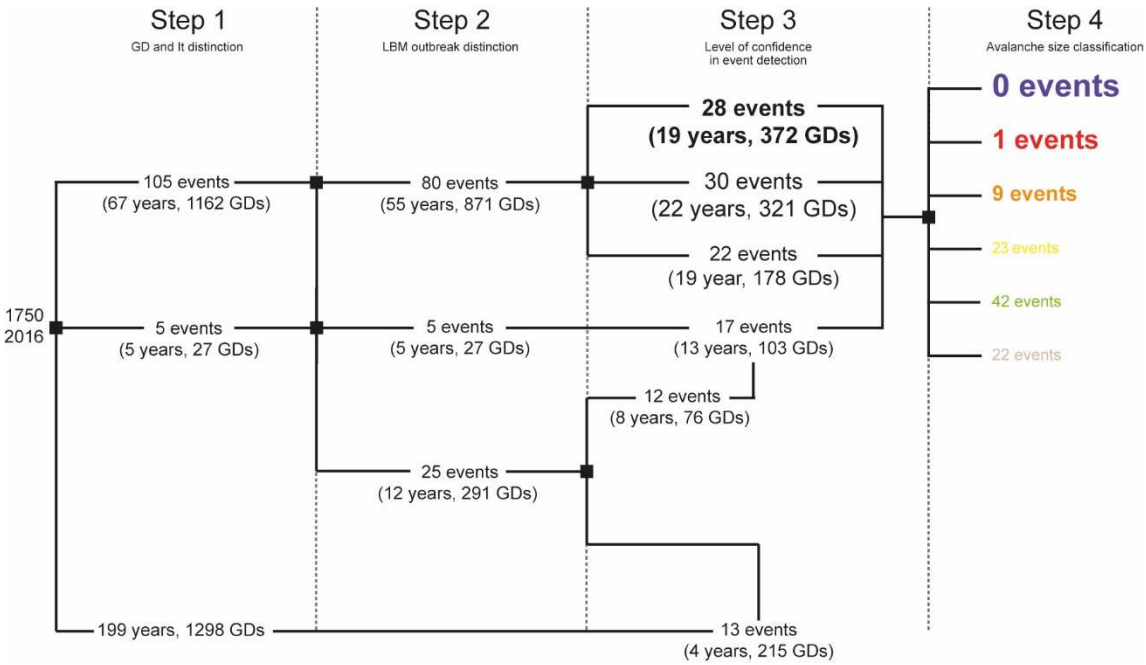

Figure 7. Synoptic diagram showing the characteristics of the reconstructed snow avalanche events and possible interferences with climate or larch budmoth outbreaks, level of confidence, and minimum slide extent.

Considering all reconstructed events, the mean recurrence interval of avalanches at Grand Bois de Souliers is 2.8 years (or 3.6 events per decade) for the period 1750–2016. The recurrence interval is not constant over time but

shows a clear decrease from 5.9 years for the periods 1750–1850 and 1851-1950 to 2 years between 1950 and 2015. Decadal frequencies reach their maximum between 1772 and 1793 (9 events), 1804–1810 (8 events), 1825-1837 (7), 1932-1937 (5), 1970-1986 (13), and 1999-2009 (10) (Fig. 8). Conversely, the number of reconstructed events decreased drastically between 1838 and 1861 (1), 1884–1900 (1), 1912–1930 (1), 1938–1959 (2), 1964–1969 (0), and 1987–1998 (5) (Fig. 8). At the path scale, the frequency of events sharply increased in A1 and A2 since 1970. In these paths, the number of reconstructed events increased from 0 to 10 and from 6 to 18 for the periods 1924-1969 and 1970-2016, respectively. By contrast, tree-ring analyses in paths S1 and S2 did not evidence any events since 1933 and 1974 whereas GDs in tree-ring series revealed only 2 avalanches with LLC in S3 since 1974 (Fig. 8). Decadal frequency of events ranged between 0.3 (S1) and 0.68 events.decade^{-1} (S4, A2) for the period 1750-1882 but is very heterogeneous between paths: while it is <0.2 event.decade^{-1} in paths A1-A2, values exceeds 1 event.decade^{-1} in S4 (1.1) and S2 (2.04) for the period 1883-2016.

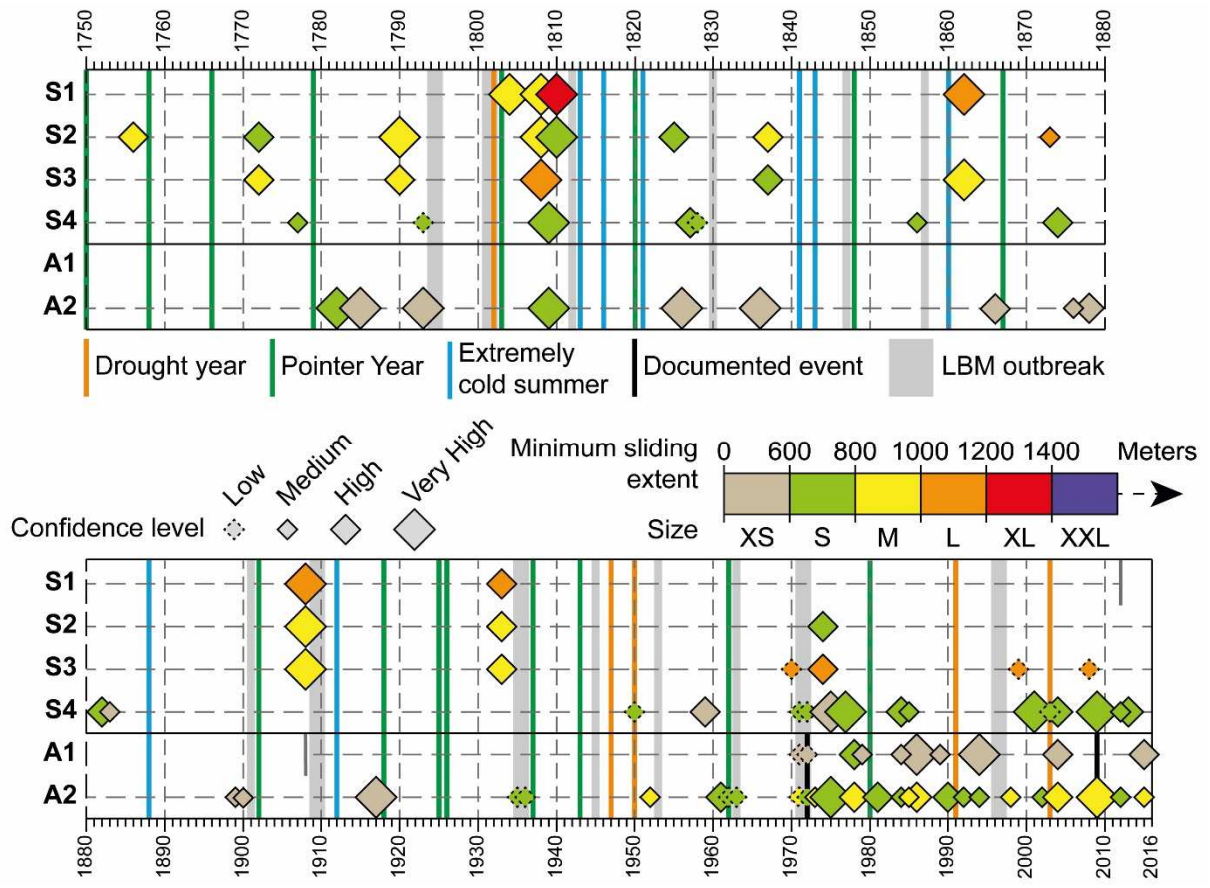

Figure 8. Avalanche events reconstructed for the period 1750–2016 in six paths at Grand Bois de Souliers. Symbol sizes are proportional to the level of confidence. The color range highlights the minimum slide extent determined from the position of impacted trees. Grey bands represent years associated to LBM outbreaks. Vertical lines show snow avalanches documented in chronicles (black), as well as extremely dry (orange) and cold (blue) summers.

5. Discussion

The study we report here employs dendrogeomorphic techniques in six avalanche paths at Grand Bois de Souliers with the aim to discuss interrelations between forests stand dynamic and snow avalanche activity as documented by tree rings. To meet this objective, we used the detection procedure developed by Favillier et al. (2017) (1) to disentangle snow avalanche signs in tree-ring records from signals induced by climatic or ecological disturbances and (2) to qualify the robustness of our tree-ring based snow avalanche reconstruction. This procedure allowed the reconstruction of 97 snow avalanche events in 67 different avalanche years back to 1750 CE. In parallel, a diachronic analysis of cartographic documents and age estimates of the stand structure allowed quantification of forest structure evolution, as well as the illustration of the afforestation process in the selected paths since the mid-18th century. In detail, our study reveals a strong dichotomy between paths S1, S2, and S3 (Group 1, G1) where the reconstructed chronology highlights the progressive disappearance of snow avalanche activity since the 1930s on one side and paths A1, A2 and to a lesser extent S4 (Group 2, G2) for which the recurrence intervals drastically increased since the 1970s on the other side. Forest cover evolution further reinforced this difference with a gradual increase in paths S1, S2, and S3 since 1750, whereas it showed an abrupt extension only around the 1920s in the other paths.

5.1 Non-stationarity of the dendrogeomorphic reconstruction potential in paths A1, A2 and S4

For the paths of Group 2, we attribute the increase in the avalanche frequency over the last decades to a non-stationarity in the potential of dendrogeomorphic approaches to capture past snow avalanches. As such, we could attribute this non-stationarity to the underestimation of hidden scars as reported by Stoffel and Perret (2006): as conifers mask scars of past events effectively, the detection and/or positioning of old scars on the stem surface remain complex, rendering determination of suitable sampling positions a difficult task. It is thus possible to miss older events on increment cores of *L. decidua*, and older trees will tend to yield data on fewer impacts relative to their age (Trappmann and Stoffel, 2013). Corona et al. (2012) evidenced that snow avalanche chronologies derived from tree-ring series tend to underestimate process activity by roughly 60%. In a more recent study, however, de Bouchard d'Aubeterre et al. (2019) demonstrated that paths covered by forests up to release zones allow to reconstruct both exhaustive—up to 70% of the real snow avalanche activity—and reliable snow avalanche chronologies over longer time periods. Accordingly, the number of reconstructed snow avalanche events must be considered as a minimum frequency in our study. As geomorphic characteristics and forest cover of the studied paths are similar to those of the Ravin de la Salce (de Bouchard d'Aubeterre et al., 2019), we consider that the reconstructed activity in our study is close to real snow avalanche activity.

Secondly, we could also attribute the tipping point observed in the reconstructions of Group2 paths in the 1970s to forest recolonization after an avalanche event destroying large parts of the forest stands, thereby removing evidence of past and subsequent events (e.g. Bryant et al., 1989; Carrara, 1989, 1979; Corona et al., 2012; Dubé et al., 2004; Germain et al., 2005; Kogelnig-Mayer et al., 2011, Larocque et al., 2001; Rayback., 1998). We could

not retrieve evidence for such an extreme event from GDs detected between 1880 and 1920 in trees from paths S4, A1 and A2. Yet, the distribution of tree ages in paths A1-A2 and S4, showing a sharp increase in sample depth during the 1930s and signs of forest recolonization on topographic maps between 1896 and 1933 (Fig. 9b, c), supports the occurrence of such an event. On the site cleared by powder-snow avalanche in 2008, *L. decidua* seedlings tend to recolonize avalanche paths at Grand Bois de Souliers within only a few years after a geomorphic event. One may therefore reasonably assume that an avalanche that would have occurred in the early 1910–1920 could have given rise to a new forest stand in the 1930s, and that this growing forest would have recovered its complete "dendrogeomorphic potential" in the 1970s. This assumption and the lags are in line with observations of a sharp increase in avalanche activity observed at Täsch (Swiss Alps; Favillier et al., 2018). Here the increase in reconstructed avalanche activity in the 1960s was the result of an extreme avalanche event that destroyed a 400×800 m forest strip in 1920. It thus seems reasonable to suggest that a forest stand will need up to 40–50 years to reach its full "dendrogeomorphic potential" after an extreme event. Obviously, the above-mentioned time period is strongly dependent of the intensity of the destructive event, the altitude of the forest stands and the recruitment rate of the considered tree species.

5.2 Non-stationarity of the snow avalanche activity related to slope afforestation

In the paths of Group 1, the frequency of GDs and avalanche events detected in the tree-ring series decreased since the 1930s. In these three paths, the oldest trees are more than 500 years old and most of the sampled trees exceed 200 years. In addition, forests continuously expanded since ca. 1540, and especially during the 18th century. The presence of multi-centennial trees in avalanche paths suggests the absence of extreme events since the mid-16th century as otherwise extreme avalanches would have destroyed the forest stand. Furthermore, evidence for more moderate snow avalanching as compared to Group2 exists via the more limited number of GDs (n=857) identified and dated in the tree-ring series from the 461 trees sampled in this sector and via the absence of injuries (intensity 4 damage). By contrast to Group1, the dendrogeomorphic potential in the paths of Group2 appears to be constant over time and reconstructions should thus properly reflect the natural fluctuations of avalanche activity. Yet, we should not dissociate conservation of the forest from human activity at Souliers. Saulnier (2012) reports that specific silvicultural rules existed since "immemorial times" at Grand Bois de Souliers to maintain the protective function of the forest stand. Interestingly, Roman (1887) and Gadoud (1917) indicate a multiplication of protective regulations between the 13th and 15th centuries in the Queyras massif aimed at preventing forest overexploitation or destruction. The proclamation of these regulations coincides with the age of the oldest trees in paths S1 and S2.

From a perspective of process dynamics, our reconstruction shows a moderate, yet continuous avalanche activity in paths S3 and S2—and to a lesser extent in S1—between the mid-18th century to the 1930s that decreased sharply thereafter. This evolution is most likely related to the afforestation of several release areas that is clearly visible through the analysis of aerial photographs since 1945. Indeed, the presence of trees is a decisive factor

stabilizing snowpack by (1) increasing terrain roughness (2) intercepting falling snow, (3) modifying radiation and temperature regimes and by (4) reducing near-surface wind speeds (de Quervain, 1978; Leitinger et al., 2008; McClung, 2003; Salm, 1978). Schneebeli and Bebi (2004) demonstrated that these effects considerably limit avalanche formation to the steepest slopes (>35°).

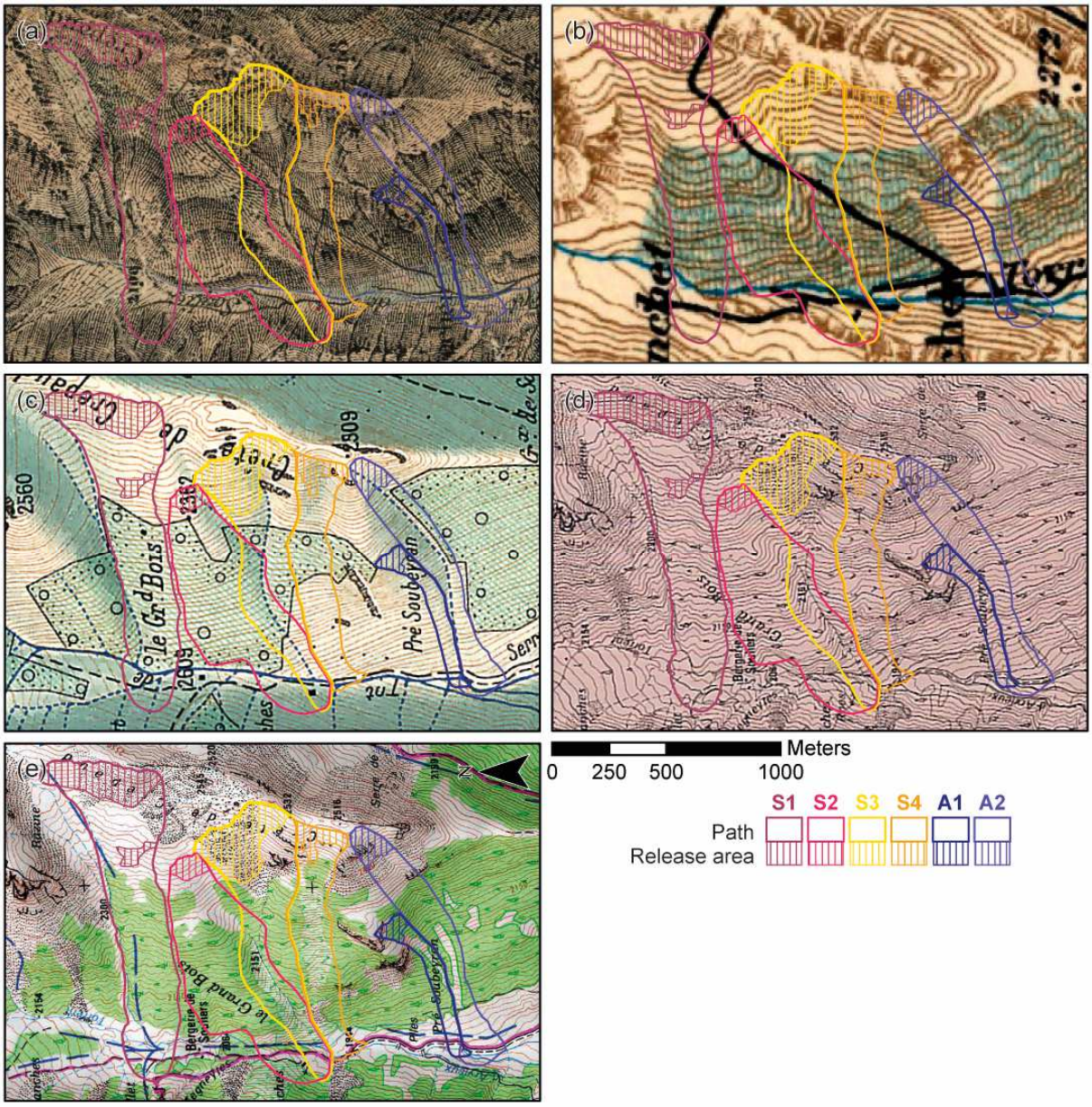

Figure 9. Diachronic comparison of topographical maps of (a) 1866, (b) 1896, (c) 1933, (d) 1971, and (e) 2015. According to the labelling system of each map, forest cover is represented by green polygons on the maps dated to (a) 1866, (b) 1896, (c) 1933 and (e) 2015, and with conifers like pictograms on (d) the 1971 map. Germination dates of sampled trees suggest that a devastating avalanche in the 1910s or 1920s cleared the forested surface in paths S1-A1-A2. Topographic maps support this interpretation by showing the absence of a forest (c) in 1933 and an almost complete (re)colonization (d) in 1971 and (e) in 2015.

Even if the interrelations between a decrease of snow avalanche activity and forest expansion are undoubted, the causes for this evolution are less easily understood. Indeed, one should keep in mind that forest colonization in paths S1-S3 dates to Medieval times as testified by the age structure of sampled trees and that the forest expanded continuously, especially during the 18th and 19th centuries. This trend is in line with the forest expansion observed at Chateau-Ville-Vieille (and at the scale of the Queyras massif), where forested areas increased from 357 ha (4400 ha in the Queyras massif) in 1747 to 2,325 ha (16,000 ha) in 1908 (Gadoud, 1917). The anthropogenic global warming cannot reasonably explain pre-industrial afforestation. According to Touflan et al. (2010) and Chauchard et al. (2010), forest and grazing management induced significant recruitment of *L. decidua* during the 18th and the 19th centuries. Larch is not only an early successional species, but also favored by shepherds because of its compatibility with grazing activities. The deciduous foliage of larch, with its soft needles and its low tree density, ensures high grass productivity and offers shelter from rain and intense sunlight to both cattle and sheep (Carrer and Urbinati, 2001; Chauchard et al., 2010; Motta and Lingua, 2005). In addition, larch is probably more resistant to trampling as compared to swiss stone pine or silver fir and its wood is also more valued for its natural decay resistance, high density and aesthetic value (Chauchard et al., 2010). In addition, the strong decrease of livestock from 6808 units (LU) in 1836 (Granet-Abisset, 1994), to 3015 LU in 1961 (Leynaud and Georges, 1965), and 1994 LU in 2010 (AGRESTE, 2012), resulting from a rural exodus (Chauchard et al., 2007; Didier, 2001; Motta and Garbarino, 2003), is an imprint of the progressive abatement of livestock grazing in the Queyras. The reduced livestock pressure and rural exodus certainly explains part of the upward shift of larch trees at Souliers as it coincides with the demographic evolutions in (1) the Chateau-Ville-Vieille municipality where the number of inhabitants decreased from 1440 in 1763 to 766 in 1911 and (2) in the Queyras massif where the 1911 census population (4094 inhabitants) was lower to the one of 1700 (5310 inhabitants) (Blanchard, 1915).

Finally, we cannot exclude potential influences of decreasing trends in snow cover depth (Beniston et al., 2018; Durand et al., 2009; Reid et al., 2016) and snow cover duration (Beniston, 1997; Uhlmann et al., 2009) on avalanche-forest interactions through direct impacts on avalanche frequency (Eckert et al., 2010c; Ballesteros-Cánovas et al., 2018) and the nature (Pielmeier et al., 2013; Naaim et al., 2016) of snow avalanches. At Grand Bois de Souliers slope, it is therefore possible that the increase in the tree-line in the 20th century was a mere bounce-back to a level without depression by previous anthropogenic activity (Gehrig-Fasel et al., 2007), rather than a climatically induced advance of the tree-line. Similarly, (i) the absence of clear trends in avalanche frequency in Group2 since the 1970s, (ii) the rather weak decrease in snow amounts and snow cover duration documented so far in the Southern French Alps (Durand et al., 2009; Castebrunet et al., 2014) at the altitudes at which the avalanche release areas are located, and (iii) the rather limited changes documented over the last decades in avalanche occurrence numbers around the study area (Eckert et al., 2013; Lavigne et al., 2015) further suggest limited impacts of global warming.

6. Conclusion

In summary, this study provided answers to the two research questions posed: (i) how does past forest cover evolution induce non-stationarities in tree-ring reconstructions of snow avalanche activity? (ii) How are trends inherent to tree-ring approaches distinguishable from real fluctuations in avalanche activity?

First, two distinct types of non-stationarities were identified in the reconstructed avalanche activity. In the three paths located in the southern part of the slope, a strong increase in avalanche frequency occurred since the 1970s. The distribution of tree ages retrieved from dendrogeomorphic analyses, in combination with old topographic maps, allowed attributing this non-stationarity to rapid afforestation of the snow avalanche paths. In the northern paths, the frequency of reconstructed events decreased in S1 during the 1930s and in S2-S3 after World War II. This non-stationarity is related to the densification of the forest stands in these paths since the 18th century and to the colonization of the release areas during the 20th century.

Second, the rapid afforestation evidenced in the three southern paths of the slope is related to a forest recolonization process induced by a snow avalanche that destroyed the forest stand before the 1930s. On the three northern paths, the identified non-stationarity indicates a decrease in snow avalanche activity induced by forest colonization processes. Even if global warming may still play a role in this evolution—by speeding up forest colonization or weakly decreasing available snow amounts in S1-S3—, both dynamics are explainable by socio-environmental factors. Their impact on forest cover dynamics, namely through forest and grazing management during the 18th century, and the rural exodus and abatement of grazing throughout the 20th century, is particularly evident.

These results demonstrate the necessity for a more careful inclusion and consideration of socio-environmental factors—such as the pastoral decline or rural exodus—to better understand and explain ongoing trends in mass-movement activity. More widely, this study calls for more systemic approaches in tree-ring reconstructions to tackle the complex interrelations among forest evolution, global warming, social practices and process activity adequately in the future.

References

AGRESTE, 2012. Recensement Agricole 2010 – Résultats – Données chiffrées. Ministère de l'Agriculture et de l'Alimentation, Paris, France.

Alestalo, J., 1971. Dendrochronological interpretation of geomorphic processes. Fennia 105, 1–139.

Ballesteros-Cánovas, J.A., Trappmann, D., Madrigal-González, J., Eckert, N., Stoffel, M., 2018. Climate warming enhances snow avalanche risk in the Western Himalayas. Proc. Natl. Acad. Sci. 115, 3410–3415. https://doi.org/10.1073/pnas.1716913115

Bebi, P., Kulakowski, D., Rixen, C., 2009. Snow avalanche disturbances in forest ecosystems–State of research and implications for management. For. Ecol. Manag. 9, 1883–1892. https:/doi.org/10.1016/j.foreco.2009.01.050

Beniston, M., 1997. Variations of Snow Depth and Duration in the Swiss Alps Over the Last 50 Years: Links to Changes in Large-Scale Climatic Forcings, in: Diaz, H.F., Beniston, M., Bradley, R.S. (Eds.), Climatic Change at High Elevation Sites. Springer Netherlands, Dordrecht, pp. 49–68. https://doi.org/10.1007/978-94-015-8905-5_3

Beniston, M., Farinotti, D., Stoffel, M., Andreassen, L.M., Coppola, E., Eckert, N., Fantini, A., Giacona, F., Hauck, C., Huss, M., Huwald, H., Lehning, M., López-Moreno, J.-I., Magnusson, J., Marty, C., Morán-Tejéda, E., Morin, S., Naaim, M., Provenzale, A., Rabatel, A., Six, D., Stötter, J., Strasser, U., Terzago, S., Vincent, C., 2018. The European mountain cryosphere: a review of its current state, trends, and future challenges. The Cryosphere 12, 759–794. https://doi.org/10.5194/tc-12-759-2018

Blanchard, R., 1915. Le Haut Dauphiné à la fin du XVIe siècle, d'après les procès-verbaux de la Révision des Feux de 1700. Rev. Géographie Alp. 3, 337–419. https://doi.org/10.3406/rga.1915.4846

Bollschweiler M., Stoffel M., Schneuwly D.M., 2008. Dynamics in debris-flow activity on a forested cone – a case study using different dendroecological approaches. Catena 72, 67–78. https://doi.org/ 10.1016/j.catena.2007.04.004

Bonnefoy, M., Barral, L., Cabos, S., Escande, S., Gaucher, R., Pasquier, X., Richard, D., 2010. The Localization Map of Avalanche Phenomena (CLPA): Stakes and Prospects. 2010 Int. Snow Sci. Workshop 699–705.

Bormann, K.J., Brown, R.D., Derksen, C., Painter, T.H., 2018. Estimating snow-cover trends from space. Nat. Clim. Change 8, 924. https://doi.org/10.1038/s41558-018-0318-3

Bosch, O. and Gutiérrez, E., 1999. La sucesión en los bosques de Pinus Ucinata del Pirineo. De los anillos de crecimiento a la historia del bosque. Ecología 13, 133–171.

Bourova, E., Maldonado, E., Leroy, J.-B., Alouani, R., Eckert, N., Bonnefoy-Demongeot, M., Deschatres, M., 2016. A new web-based system to improve the monitoring of snow avalanche hazard in France. Nat. Hazards Earth Syst. Sci. 16, 1205–1216. https://doi.org/10.5194/nhess-16-1205-2016

Butler, D.R., Sawyer, C.F., 2008. Dendrogeomorphology and high-magnitude snow avalanches: a review and case study. Nat. Hazards Earth Syst. Sci. 8, 303–309. https://doi.org/10.5194/nhess-8-303-2008

Bryant, C.L., Butler, D.R., Vitek, J.D., 1989. A statistical analysis of tree-ring dating in conjunction with snow avalanches: Comparison of on-path versus off-path responses. Environ. Geol. Water S. 14, 53–59. https://doi.org/10.1007/BF01740585

Carrara, P.E., 1979. The determination of snow avalanche frequency through tree-ring analysis and historical records at Ophir, Colorado. Geol. Soc. Am. Bull. 90, 773–780. https://doi.org/10.1130/0016-7606(1979)90<773:TDOSAF>2.0.CO;2

Carrara, P.E., 1989. Late quaternary glacial and vegetative history of the Glacier National Park region, Montana (USGS Numbered Series No. 1902), Bulletin. U.S. G.P.O. ; For sale by the Books and Open-File Reports Section, U.S. Geological Survey,.

Carrer, M., Urbinati, C., 2001. Assessing climate-growth relationships: a comparative study between linear and non-linear methods. Dendrochronologia 1, 57–65.

Castebrunet, H., Eckert, N., Giraud, G., 2012. Snow and weather climatic control on snow avalanche occurrence fluctuations over 50 yr in the French Alps. Clim Past 8, 855–875. https://doi.org/10.5194/cp-8-855-2012

Castebrunet, H., Eckert, N., Giraud, G., Durand, Y., Morin, S., 2014. Projected changes of snow conditions and avalanche activity in a warming climate: a case study in the French Alps over the 2020–2050 and 2070–2100 periods. Cryosphere Discuss 8, 581–640. https://doi.org/10.5194/tcd-8-581-2014

Chauchard, S., Beilhe, F., Denis, N., Carcaillet, C., 2010. An increase in the upper tree-limit of silver fir (Abies alba Mill.) in the Alps since the mid-20th century: A land-use change phenomenon. For. Ecol. Manag. 259, 1406–1415. https://doi.org/10.1016/j.foreco.2010.01.009

Chauchard, S., Carcaillet, C., Guibal, F., 2007. Patterns of Land-use Abandonment Control Tree-recruitment and Forest Dynamics in Mediterranean Mountains. Ecosystems 10, 936–948. https://doi.org/10.1007/s10021-007-9065-4

Chimani, B., Matulla, C., Böhm, R., Hofstätter, M., 2013. A new high resolution absolute temperature grid for the Greater Alpine Region back to 1780. Int. J. Climatol. 33, 2129–2141. https://doi.org/10.1002/joc.3574

Corona, C., Lopez Saez, J., Stoffel, M., Bonnefoy, M., Richard, D., Astrade, L., Berger, F., 2012. How much of the real avalanche activity can be captured with tree rings? An evaluation of classic dendrogeomorphic

518 approaches and comparison with historical archives. Cold Reg. Sci. Technol. 74–75, 31–42.
519 https://doi.org/10.1016/j.coldregions.2012.01.003

520 Corona, C., Saez, J.L., Stoffel, M., Rovéra, G., Edouard, J.-L., Berger, F., 2013. Seven centuries of avalanche
521 activity at Echalp (Queyras massif, southern French Alps) as inferred from tree rings. The Holocene 23,
522 292–304. https://doi.org/10.1177/0959683612460784

523 Coughlan, M.R., 2013. Errakina: Pastoral Fire Use and Landscape Memory In the Basque Region of the French
524 Western Pyrenees. J. Ethnobiol. 33, 86–104. https://doi.org/10.2993/0278-0771-33.1.86

525 de Quervain, M., 1978. Wald und Lawinen, in: Proceedings of the IUFRO. Presented at the Seminar Mountain
526 Forests and Avalanches, Davos, Switzerland, pp. 219–231.

527 Desloges, J.R., Ryder, J.M., 1990. Neoglacial history of the Coast Mountains near Bella Coola, British Columbia.
528 Can. J. Earth Sci. 27, 281–290. https://doi.org/10.1139/e90-027

529 Didier, L., 2001. Invasion patterns of European larch and Swiss stone pine in subalpine pastures in the French Alps.
530 For. Ecol. Manag. 145, 67–77. https://doi.org/10.1016/S0378-1127(00)00575-2

531 Dubé, S., Filion, L., Hétu, B., 2004. Tree-ring reconstruction of high-magnitude snow avalanches in Gaspé
532 Péninsula, Québec, Canada. Arct. Antarct. Alp. Res. 36, 555–564. https://10.1657/1523-
533 0430(2004)036[0555:TROHSA]2.0.CO:2

534 Durand, Y., Giraud, G., Laternser, M., Etchevers, P., Mérindol, L., Lesaffre, B., 2009. Reanalysis of 47 Years of
535 Climate in the French Alps (1958–2005): Climatology and Trends for Snow Cover. J. Appl. Meteorol.
536 Climatol. 48, 2487–2512. https://doi.org/10.1175/2009JAMC1810.1

537 Eckert, N., Baya, H., Deschatres, M., 2010a. Assessing the Response of Snow Avalanche Runout Altitudes to
538 Climate Fluctuations Using Hierarchical Modeling: Application to 61 Winters of Data in France. J. Clim. 23,
539 3157–3180. https://doi.org/10.1175/2010JCLI3312.1

540 Eckert, N., Coleou, C., Castebrunet, H., Deschatres, M., Giraud, G., Gaume, J., 2010b. Cross-comparison of
541 meteorological and avalanche data for characterising avalanche cycles: The example of December 2008
542 in the eastern part of the French Alps. Cold Reg. Sci. Technol. 64, 119–136.
543 https://doi.org/10.1016/j.coldregions.2010.08.009

544 Eckert, N., Parent, E., Kies, R., Baya, H., 2010c. A spatio-temporal modelling framework for assessing the
545 fluctuations of avalanche occurrence resulting from climate change: application to 60 years of data in the
546 northern French Alps. Clim. Change 101, 515–553. https://doi.org/10.1007/s10584-009-9718-8

Eckert, N., Keylock, C.J., Castebrunet, H., Lavigne, A., Naaim, M., 2013. Temporal trends in avalanche activity in the French Alps and subregions: from occurrences and runout altitudes to unsteady return periods. J. Glaciol. 59, 93–114. https://doi.org/10.3189/2013JoG12J091

Efthymiadis, D., Jones, P.D., Briffa, K.R., Auer, I., Böhm, R., Schöner, W., Frei, C., Schmidli, J., 2006. Construction of a 10-min-gridded precipitation data set for the Greater Alpine Region for 1800–2003. J. Geophys. Res. 111. https://doi.org/10.1029/2005JD006120

ESRI, 2013. ArcGIS 10.2.1. ESRI, Redlands, CA.

Eynard-Machet, R., 1993. Anciens cadastres et évolution des paysages. Cartographie historique de l'occupation des sols dans les Alpes de Savoie, France. Rev. Géographie Alp. 81, 51–66. https://doi.org/10.3406/rga.1993.3719

Falarz, M., 2004. Variability and trends in the duration and depth of snow cover in Poland in the 20th century. Int. J. Climatol. 24, 1713–1727. https://doi.org/10.1002/joc.1093

Favillier, A., Guillet, S., Morel, P., Corona, C., Lopez-Saez, J., Eckert, N., Ballesteros Cánovas, J.A., Peiry, J.-L., Stoffel, M., 2017. Disentangling the impacts of exogenous disturbances on forest stands to assess multi-centennial tree-ring reconstructions of avalanche activity in the upper Goms Valley (Canton of Valais, Switzerland). Quat. Geochronol. 42, 89–104. https://doi.org/10.1016/j.quageo.2017.09.001

Favillier, A., Guillet, S., Trappmann, D., Morel, P., Lopez-Saez, J., Eckert, N., Zenhäusern, G., Peiry, J.-L., Stoffel, M., Corona, C., 2018. Spatio-temporal maps of past avalanche events derived from tree-ring analysis: A case study in the Zermatt valley (Valais, Switzerland). Cold Reg. Sci. Technol. 154, 9–22. https://doi.org/10.1016/j.coldregions.2018.06.004

Gądek, B., Kaczka, R.J., Rączkowska, Z., Rojan, E., Casteller, A., Bebi, P., 2017. Snow avalanche activity in Żleb Żandarmerii in a time of climate change (Tatra Mts., Poland). CATENA 158, 201–212. https://doi.org/10.1016/j.catena.2017.07.005

Gadoud, M., 1917. Les forêts du Haut-Dauphiné a la fin du XVIIe siècle et de nos jours. Imprimerie Allier Frère, Grenoble.

García-Hernández, C., Ruiz-Fernández, J., Sánchez-Posada, C., Pereira, S., Oliva, M., Vieira, G., 2017. Reforestation and land use change as drivers for a decrease of avalanche damage in mid-latitude mountains (NW Spain). Glob. Planet. Change 153, 35–50. https://doi.org/10.1016/j.gloplacha.2017.05.001

Gaucher, R., Pasquier, X., Bonnefoy, M., Eckert, N., Deschatres, M., 2009. Quelques exemples d'avalanches exceptionelles. Neige Avalanche 10–14.

577 Gehrig-Fasel, J., Guisan, A., Zimmermann, N.E., 2007. Tree line shifts in the Swiss Alps: Climate change or land
578 abandonment? J. Veg. Sci. 18, 571–582. https://doi.org/10.1111/j.1654-1103.2007.tb02571.x

579 Gellrich, M., Baur, P., Koch, B., Zimmermann, N.E., 2007. Agricultural land abandonment and natural forest re-
580 growth in the Swiss mountains: A spatially explicit economic analysis. Agric. Ecosyst. Environ. 118, 93–
581 108. https://doi.org/10.1016/j.agee.2006.05.001

582 Germain, D., Filion, L., Hétu, B., 2005. Snow avalanche activity after fire and logging disturbances, northern Gaspé
583 Peninsula, Quebec, Canada. Can. J. Earth Sci. 42, 2103–2116. https://doi.org/10.1139/E05-087

584 Giacona, F., Eckert, N., Mainieri, R., Martin, B., Corona, C., Lopez-Saez, J., Monnet, J.-M., Naaim, M., Stoffel, M.,
585 2018. Avalanche activity and socio-environmental changes leave strong footprints in forested landscapes:
586 a case study in the Vosges medium-high mountain range. Ann. Glaciol. 1–23.
587 https://doi.org/10.1017/aog.2018.26

588 Giacona, F., Eckert, N., Martin, B., 2017. A 240-year history of avalanche risk in the Vosges Mountains based on
589 non-conventional (re)sources. Nat Hazards Earth Syst Sci 17, 887–904. https://doi.org/10.5194/nhess-17-
590 887-2017

591 Granet-Abisset, A.-M., 1994. La route réinventée : les migrations des Queyrassins aux XIXe et XXe siècles, La
592 pierre et l'écrit. Presses universitaires de Grenoble, Grenoble.

593 Hétu, B., Fortin, G., Brown, N., 2015. Climat hivernal, aménagement du territoire et dynamique des avalanches au
594 Québec méridional : une analyse à partir des accidents connus depuis 1825. Can. J. Earth Sci. 52, 307–
595 321. https://doi.org/10.1139/cjes-2014-0205

596 Houghton, R.A., House, J.I., Pongratz, J., van der Werf, G.R., DeFries, R.S., Hansen, M.C., Le Quéré, C.,
597 Ramankutty, N., 2012. Carbon emissions from land use and land-cover change. Biogeosciences 9, 5125–
598 5142. https://doi.org/10.5194/bg-9-5125-2012

599 IPCC, 2013. Climate Change 2013: The Physical Science Basis. Contribution of Working Group I to the Fifth
600 Assessment Report of the Intergovernmental Panel on Climate Change, Cambridge University Press. ed.
601 Intergovernmental Panel on Climate Change, Cambridge, United Kingdom ; New York, NY, USA.

602 Kajimoto, T., Daimaru, H., Okamoto, T., Otani, T., Onodera, H., 2004. Effects of Snow Avalanche Disturbance on
603 Regeneration of Subalpine Abies mariesii Forest, Northern Japan. Arct. Antarct. Alp. Res. 36, 436–445.
604 https://doi.org/10.1657/1523-0430(2004)036[0436:EOSADO]2.0.CO;2

605 Kennedy, M., 2013. Introducing geographic information systems with ArcGIS: a workbook approach to learning
606 GIS, Third edition. ed. John Wiley & Sons, Hoboken, New Jersey.

607 Koch, J., 2009. Improving age estimates for late Holocene glacial landforms using dendrochronology – Some
608 examples from Garibaldi Provincial Park, British Columbia. Quat. Geochronol. 4, 130–139.
609 https://doi.org/10.1016/j.quageo.2008.11.002

610 Kogelnig-Mayer, B., Stoffel, M., Schneuwly-Bollschweiler, M., 2013. Four-dimensional growth response of mature
611 Larix decidua to stem burial under natural conditions. Trees 27, 1217–1223.
612 https://doi.org/10.1007/s00468-013-0870-4

613 Kogelnig-Mayer, B., Stoffel, M., Schneuwly-Bollschweiler, M., Hübl, J., Rudolf-Miklau, F., 2011. Possibilities and
614 Limitations of Dendrogeomorphic Time-Series Reconstructions on Sites Influenced by Debris Flows and
615 Frequent Snow Avalanche Activity. Arct. Antarct. Alp. Res. 43, 649–658. https://doi.org/10.1657/1938-
616 4246-43.4.649

617 Köhler, A., Fischer, J.-T., Scandroglio, R., Bavay, M., McElwaine, J., Sovilla, B., 2018. Cold-to-warm flow regime
618 transition in snow avalanches. The Cryosphere 12, 3759–3774. https://doi.org/10.5194/tc-12-3759-2018

619 Kulakowski, D., Rixen, C., Bebi, P., 2006. Changes in forest structure and in the relative importance of climatic
620 stress as a result of suppression of avalanche disturbances. Forest Ecol. Manag. 223, 66–74.
621 https://doi.org/10.1016/j.foreco.2005.10.058

622 Kulakowski D., Bebi, P., Rixen, C., 2011. The interacting effects of land use change, climate change and
623 suppression of natural disturbances on landscape forest structure in the Swiss Alps. Oikos 120, 216–225.
624 https://doi.org/10.1111/j.1600-0706.2010.18726.x

625 Larocque, S.J., Hétu, B., Filion, L., 2001. Geomorphic and dendroecological impacts of slushflows in central Gaspé
626 Peninsula (Québec, Canada). Geogr. Ann. 83A, 191–201. https://doi.org/10.1111/j.0435-
627 3676.2001.00154.x

628 Larsson, L.A., 2016. CDendro — Cybis Dendro Dating Program. Cybis Elektron. Data AB Saltsjöbaden Swed.

629 Laternser, M., Schneebeli, M., 2003. Long-term snow climate trends of the Swiss Alps (1931-99). Int. J. Climatol.
630 23, 733–750. https://doi.org/10.1002/joc.912

631 Lavigne, A., Eckert, N., Bel, L., Parent, E., 2015. Adding expert contributions to the spatiotemporal modelling of
632 avalanche activity under different climatic influences. J. R. Stat. Soc. Ser. C Appl. Stat. 64, 651–671.
633 https://doi.org/10.1111/rssc.12095

634 Leitinger, G., Höller, P., Tasser, E., Walde, J., Tappeiner, U., 2008. Development and validation of a spatial snow-
635 glide model. Ecol. Model. 211, 363–374. https://doi.org/10.1016/j.ecolmodel.2007.09.015

636 Lewis, D., Smith, D., 2004. Dendrochronological Mass Balance Reconstruction, Strathcona Provincial Park,
637 Vancouver Island, British Columbia, Canada. Arct. Antarct. Alp. Res. 36, 598–606.
638 https://doi.org/10.1657/1523-0430(2004)036[0598:DMBRSP]2.0.CO;2

639 Leynaud, E., Georges, M., 1965. Aspects géographiques de l'élevage dans la zone de montagne du département
640 des Hautes-Alpes. Études Rural. 18, 5–36. https://doi.org/10.3406/rural.1965.1214

641 MacDonald, D., Crabtree, J.R., Wiesinger, G., Dax, T., Stamou, N., Fleury, P., Gutierrez Lazpita, J., Gibon, A.,
642 2000. Agricultural abandonment in mountain areas of Europe: Environmental consequences and policy
643 response. J. Environ. Manage. 59, 47–69. https://doi.org/10.1006/jema.1999.0335

644 Malanson, G.P., Butler, D.R., 1984. Transverse pattern of vegetation on avalanche paths in the northern Rocky
645 Mountains, Montana. Gt. Basin Nat. 44, 453–458.

646 Marty, C., Tilg, A.-M., Jonas, T., 2017. Recent Evidence of Large-Scale Receding Snow Water Equivalents in the
647 European Alps. J. Hydrometeorol. 18, 1021–1031. https://doi.org/10.1175/JHM-D-16-0188.1

648 McCarthy, D.P., Luckman, B.H., Kelly, P.E., 1991. Sampling Height-Age Error Correction for Spruce Seedlings in
649 Glacial Forefields, Canadian Cordillera. Arct. Alp. Res. 23, 451–455. https://doi.org/10.2307/1551687

650 McClung, D.M., 2003. Magnitude and Frequency of Avalanches in Relation to Terrain and Forest Cover. Arct.
651 Antarct. Alp. Res. 35, 82–90. https://doi.org/10.1657/1523-0430(2003)035[0082:MAFOAI]2.0.CO;2

652 Morán-Tejeda, E., López-Moreno, J.I., Beniston, M., 2013. The changing roles of temperature and precipitation on
653 snowpack variability in Switzerland as a function of altitude: role of altitude on swiss snowpack. Geophys.
654 Res. Lett. 40, 2131–2136. https://doi.org/10.1002/grl.50463

655 Motta, R., Garbarino, F., 2003. Stand history and its consequences for the present and future dynamic in two silver
656 fir (*Abies alba* Mill.) stands in the high Pesio Valley (Piedmont, Italy). Ann. For. Sci. 60, 361–370.
657 https://doi.org/10.1051/forest:2003027

658 Motta, R., Lingua, E., 2005. Human impact on size, age, and spatial structure in a mixed European larch and Swiss
659 stone pine forest in the Western Italian Alps. Can. J. For. Res. 35, 1809–1820. https://doi.org/10.1139/x05-
660 107

661 Mougin, P., 1922. Les avalanches en Savoie. Ministère de l'Agriculture, Direction Générale des Eaux et Forêts,
662 Service des Grandes Forces Hydrauliques, Paris.

663 Mountain Research Initiative EDW Working Group, Pepin, N., Bradley, R.S., Diaz, H.F., Baraer, M., Caceres, E.B.,
664 Forsythe, N., Fowler, H., Greenwood, G., Hashmi, M.Z., Liu, X.D., Miller, J.R., Ning, L., Ohmura, A.,
665 Palazzi, E., Rangwala, I., Schöner, W., Severskiy, I., Shahgedanova, M., Wang, M.B., Williamson, S.N.,

Yang, D.Q., 2015. Elevation-dependent warming in mountain regions of the world. Nat. Clim. Change 5, 424–430. https://doi.org/10.1038/nclimate2563

Muntán, E., Andreu, L., Oller, P., Gutiérrez, E. and Martínez, P., 2004. Dendrochronological study of the Canal del Roc Roig avalanche path: first results of the Aludex project in the Pyrenees. Ann. Glaciol. 38, 173–179. https://doi.org/10.3189/172756404781815077

Naaim, M., Durand, Y., Eckert, N., Chambon, G., 2013. Dense avalanche friction coefficients: influence of physical properties of snow. J. Glaciol. 59(216), 771–782. https://doi.org/10.3189/2013JoG12J205

Naaim, M., Eckert, N., Giraud, G., Faug, T., Chambon, G., Naaim-Bouvet, F., Richard, D., 2016. Impact du réchauffement climatique sur l'activité avalancheuse et multiplication des avalanches humides dans les Alpes françaises. Houille Blanche 12–20. https://doi.org/10.1051/lhb/2016055

O'Rourke, E., 2006. Changes in agriculture and the environment in an upland region of the Massif Central, France. Environ. Sci. Policy, European Rural Landscapes: Land-use, biodiversity, and conservation 9, 370–375. https://doi.org/10.1016/j.envsci.2006.01.008

Pielmeier, C., Techel, F., Marty, C., Stucki, T., 2013. Wet snow avalanche activity in the Swiss Alps - trend analysis for mid-winter season. Proc. Int. Snow Sci. Workshop 1240–1246.

Podolskiy, E.A., Izumi, K., Suchkov, V.E., Eckert, N., 2014. Physical and societal statistics for a century of snow-avalanche hazards on Sakhalin and Kuril Islands (1910–2010). J. Glaciol. 221, 409–430. https://doi.org/10.3189/2014/JoG13J143

Rayback, S.A., 1998. A dendrogeomorphological analysis of snow avalanches in the Colorado Front Range, USA. Phys. Geogr. 19, 502–515. https://doi.org/10.1080/02723646.1998.10642664

Reid, P.C., Hari, R.E., Beaugrand, G., Livingstone, D.M., Marty, C., Straile, D., Barichivich, J., Goberville, E., Adrian, R., Aono, Y., Brown, R., Foster, J., Groisman, P., Hélaouët, P., Hsu, H.-H., Kirby, R., Knight, J., Kraberg, A., Li, J., Lo, T.-T., Myneni, R.B., North, R.P., Pounds, J.A., Sparks, T., Stübi, R., Tian, Y., Wiltshire, K.H., Xiao, D., Zhu, Z., 2016. Global impacts of the 1980s regime shift. Glob. Change Biol. 22, 682–703. https://doi.org/10.1111/gcb.13106

Roman, J., 1887. Les causes du déboisement des montagnes, d'après les documents historiques du XIIIe au XVIIIe siècle. Imprimerie J.-C. Richaud, Gap.

Salm, B., 1978. Snow forces on forest plants, in: In der Gand, H., Kronfeller, G., Ott, E., Salm, B. (Eds.), International Seminar on Mountain Forests and Avalanches. Presented at the IUFRO Working Party on Snow and Avalanches, Swiss Federal Institute for Snow and Avalanche Research, Davos, Switzerland, pp. 156–181.

Saulnier, M., 2012. Histoire et dynamique de la forêt subalpine dans les Alpes du Sud (Briançonnais, Queyras) : approches pédoanthracologique et dendrochronologique (thesis). Aix-Marseille Université, Aix-en-Provence, 392 pp.

Saulnier, M., Corona, C., Stoffel, M., Guibal, F., Edouard, J.-L., 2019. Climate-growth relationships in a Larix decidua Mill. network in the French Alps. Sci. Total Environ. 664, 554–566. https://doi.org/10.1016/j.scitotenv.2019.01.404

Saulnier, M., Edouard, J.-L., Corona, C., Guibal, F., 2011. Climate/growth relationships in a Pinus cembra high-elevation network in the Southern French Alps. Ann. For. Sci. 68, 189–200. https://doi.org/10.1007/s13595-011-0020-3

Saulnier, M., Roques, A., Guibal, F., Rozenberg, P., Saracco, G., Corona, C., Edouard, J.-L., 2017. Spatiotemporal heterogeneity of larch budmoth outbreaks in the French Alps over the last 500 years. Can. J. For. Res. 47, 667–680. https://doi.org/10.1139/cjfr-2016-0211

Saulnier, M., Talon, B., Edouard, J.-L., 2015. New pedoanthracological data for the long-term history of forest species at mid-high altitudes in the Queyras Valley (Inner Alps). Quat. Int., Charcoal: resource and ubiquitous proxy 366, 15–24. https://doi.org/10.1016/j.quaint.2014.11.023

Schneebeli, M., Bebi, P., 2004. Snow and avalanche control, in: Burley, J., Evans, J., Youngquist, J.A. (Eds.), Encyclopedia of Forest Sciences. pp. 397–402.

Schneuwly, D.M., Stoffel, M., Bollschweiler, M., 2009a. Formation and spread of callus tissue and tangential rows of resin ducts in Larix decidua and Picea abies following rockfall impacts. Tree Physiol. 29, 281–289. https://doi.org/10.1093/treephys/tpn026

Schneuwly, D.M., Stoffel, M., Dorren, L.K.A., Berger, F., 2009b. Three-dimensional analysis of the anatomical growth response of European conifers to mechanical disturbance. Tree Physiol. 29, 1247–1257. https://doi.org/10.1093/treephys/tpp056

Shroder, J.F., 1978. Dendrogeomorphological Analysis of Mass Movement on Table Cliffs Plateau, Utah. Quat. Res. 9, 168–185. https://doi.org/10.1016/0033-5894(78)90065-0

Šilhán, K., Stoffel, M., 2015. Impacts of age-dependent tree sensitivity and dating approaches on dendrogeomorphic time series of landslides. Geomorphology 236, 34–43. https://doi.org/10.1016/j.geomorph.2015.02.003

Sorg, A., Bugmann, H., Bollschweiler, M., Stoffel, M., 2010. Debris-flow activity along a torrent in the Swiss Alps: Minimum frequency of events and implications for forest dynamics. Dendrochronologia 28, 215–223. https://doi.org/10.1016/j.dendro.2009.11.002

727 Stoffel, M., Bollschweiler, M., 2008. Tree-ring analysis in natural hazards research – an overview. Nat. Hazards
728 Earth Syst. Sci. 187–202.

729 Stoffel, M., Corona, C., 2018. Future winters glimpsed in the Alps. Nat. GeoSci. 11, 458–460. https://doi.org/
730 10.1038/s41561-018-0177-6

731 Stoffel, M., Huggel, C., 2012. Effects of climate change on mass movements in mountain environments. Prog. Phys.
732 Geog. 36, 421–439. https://doi.org/ 10.1177/0309133312441010

733 Stoffel, M., Bollschweiler, M., Butler, D.R., Luckman, B.H., 2010. Tree rings and natural hazards: A State-of-the-
734 Art. Springer.

735 Stoffel, M., Bollschweiler, M., Hassler, G.-R., 2006. Differentiating past events on a cone influenced by debris-flow
736 and snow avalanche activity – a dendrogeomorphological approach. Earth Surf. Process. Landf. 31, 1424–
737 1437. https://doi.org/10.1002/esp.1363

738 Stoffel, M., Butler, D.R., Corona, C., 2013. Mass movements and tree rings: A guide to dendrogeomorphic field
739 sampling and dating. Geomorphology 200, 106–120. https://doi.org/10.1016/j.geomorph.2012.12.017

740 Stoffel, M., Corona, C., 2014. Dendroecological Dating of Geomorphic Disturbance in Trees. Tree-Ring Res. 70,
741 3–20. https://doi.org/10.3959/1536-1098-70.1.3

742 Stoffel, M., Perret, S., 2006. Reconstructing past rockfall activity with tree rings: Some methodological
743 considerations. Dendrochronologia 1–15. https://doi.org/10.1016/j.dendro.2006.04.001

744 Teich, M., Marty, C., Gollut, C., Grêt-Regamey, A., Bebi, P., 2012. Snow and weather conditions associated with
745 avalanche releases in forests: Rare situations with decreasing trends during the last 41years. Cold Reg.
746 Sci. Technol. 83–84, 77–88. https://doi.org/10.1016/j.coldregions.2012.06.007

747 Touflan, P., Talon, B., Walsh, K., 2010. Soil charcoal analysis: a reliable tool for spatially precise studies of past
748 forest dynamics: a case study in the French southern Alps. The Holocene 20, 45–52.
749 https://doi.org/10.1177/0959683609348900

750 Trappmann, D., Stoffel, M., 2013. Counting scars on tree stems to assess r—ockfall hazards: A low effort approach,
751 but how reliable? Geomorphology 180–181, 180–186. https://doi.org/10.1016/j.geomorph.2012.10.009

752 Uhlmann, B., Goyette, S., Beniston, M., 2009. Sensitivity analysis of snow patterns in Swiss ski resorts to shifts in
753 temperature, precipitation and humidity under conditions of climate change. Int. J. Climatol. 29, 1048–
754 1055. https://doi.org/10.1002/joc.1786

755 Van der Burght, L., Stoffel, M., Bigler, C., 2012. Analysis and modelling of tree succession on a recent rockslide
756 deposit. Plant Ecol. 213, 35–46. https://doi.org/10.1007/s11258-011-0004-2

Yoshida, K., Kikuchi, S., Nakamura, F., Noda, M., 1997. Dendrochronological analysis of debris flow disturbance on Rishiri Island. Geomorphology 20, 135–145. https://doi.org/10.1016/S0169-555X(97)00010-X

Captions

Figure 1. Location of the studied paths: (a) overview of the Queyras massif (French Alps), (b) detailed view of the Chateau-Ville-Vieille locality within the Queyras massif and the study site (c) detailed view of the six avalanche paths delineated on the Grand Bois de Souliers slope.

Figure 2. Synoptic diagram of the 4-step approach used for the detection of avalanche events in tree-ring series, adapted from Favillier et al. (2017). Growth disturbance (GD) and Shroder's It index (It) thresholds vary according to sample size: (a) <20 trees; (b) 20 to 49 trees; (c) 50 to 99 trees; and (d) ≥ 100 trees. We analyzed avalanche events occurring at the same time as larch budmoth outbreaks (LBM) or climatic events again and assigned confidence levels to these events according to the weighted index factor (Wit).

Figure 3. Age structure of the forest stand growing at Grand Bois de Souliers: (a) spatial distribution of individual tree and interpolated stand ages; (b) evolution of the sample size at the six avalanche paths. The black line represents the mean sample size evolution.

Figure 4. Diachronic evolution of the forest stands at Grand Bois de Souliers between 1945 and 2015: (a) 1945-1971, (b) 1971-1981, (c) 1981-2003, and (d) 2003-2015.

Figure 5. Evolution of the surfaces occupied by larch stands, computed for 100-m elevation bands, (a) at Grand Bois de Souliers; within (b) avalanche paths S1-S3; and (c) paths S4, A1 and A2 as delineated in Fig. 1.

Figure 6. Barplots showing the distributions of GD types and intensities between 1750 and 2000 for paths (a) S1-S3 and (b) S4-A1-A2.

Figure 7. Synoptic diagram showing the characteristics of the reconstructed snow avalanche events and possible interferences with climate or larch budmoth outbreaks, level of confidence, and minimum slide extent.

Figure 8. Avalanche events reconstructed for the period 1750–2016 in six paths at Grand Bois de Souliers. Symbol sizes are proportional to the level of confidence. The color range highlights the minimum slide extent determined from the position of impacted trees. Grey bands represent years associated to LBM outbreaks. Vertical lines show snow avalanches documented in chronicles (black), as well as extremely dry (orange) and cold (blue) summers.

Figure 9. Diachronic comparison of topographical maps of (a) 1866, (b) 1896, (c) 1933, (d) 1971, and (e) 2015. According to the labelling system of each map, forest cover is represented by green polygons on the maps dated to (a) 1866, (b) 1896, (c) 1933 and (e) 2015, and with conifers like pictograms on (d) the 1971 map. Germination dates of sampled trees suggest that a devastating avalanche in the 1910s or 1920s cleared the forested surface in

paths S1-A1-A2. Topographic maps support this interpretation by showing the absence of a forest (c) in 1933 and an almost complete (re)colonization (d) in 1971 and (e) in 2015.

Table 1. Main characteristics of the studied avalanche paths. Numerical values correspond to the areas delineated in Fig. 1c and derived from crossed a 5-m DEM.

Table 2. Larch budmoth years (in bold) and pointer years (in italics) – according to Saulnier et al. (2017) – as well as extremely cold (*) and dry summers (**) (Efthymiadis et al., 2006; Saulnier et al., 2011) recorded in the French Alps. A careful analysis of these years enables detection of possible interferences between snow avalanche damage in trees and LBM and/or climatic signals. Both LBM and climate events may induce growth reductions comparable to those observed after snow avalanches in the tree-ring series.

Table 3. Intensities of reactions and types of growth disturbances (GD) assessed in the 825 larch trees selected for analysis.